

Spring 1999

Isolation and characterization of a *Caenorhabditis elegans* SRC loss-of-function allele using reverse genetics

Jennifer Dignan Hogan
University of New Hampshire, Durham

Follow this and additional works at: <https://scholars.unh.edu/dissertation>

Recommended Citation

Hogan, Jennifer Dignan, "Isolation and characterization of a *Caenorhabditis elegans* SRC loss-of-function allele using reverse genetics" (1999). *Doctoral Dissertations*. 2071.
<https://scholars.unh.edu/dissertation/2071>

This Dissertation is brought to you for free and open access by the Student Scholarship at University of New Hampshire Scholars' Repository. It has been accepted for inclusion in Doctoral Dissertations by an authorized administrator of University of New Hampshire Scholars' Repository. For more information, please contact nicole.hentz@unh.edu.

INFORMATION TO USERS

This manuscript has been reproduced from the microfilm master. UMI films the text directly from the original or copy submitted. Thus, some thesis and dissertation copies are in typewriter face, while others may be from any type of computer printer.

The quality of this reproduction is dependent upon the quality of the copy submitted. Broken or indistinct print, colored or poor quality illustrations and photographs, print bleedthrough, substandard margins, and improper alignment can adversely affect reproduction.

In the unlikely event that the author did not send UMI a complete manuscript and there are missing pages, these will be noted. Also, if unauthorized copyright material had to be removed, a note will indicate the deletion.

Oversize materials (e.g., maps, drawings, charts) are reproduced by sectioning the original, beginning at the upper left-hand corner and continuing from left to right in equal sections with small overlaps. Each original is also photographed in one exposure and is included in reduced form at the back of the book.

Photographs included in the original manuscript have been reproduced xerographically in this copy. Higher quality 6" x 9" black and white photographic prints are available for any photographs or illustrations appearing in this copy for an additional charge. Contact UMI directly to order.

UMI

**A Bell & Howell Information Company
300 North Zeeb Road, Ann Arbor MI 48106-1346 USA
313/761-4700 800/521-0600**

.

**ISOLATION AND CHARACTERIZATION OF A
CAENORHABDITIS ELEGANS
SRC LOSS-OF-FUNCTION ALLELE USING REVERSE GENETICS**

BY

**JENNIFER DIGNAN HOGAN
B.S., University of Michigan - Flint, 1994**

**John J. Collins - Dissertation Advisor
Assistant Professor
Department of Biochemistry and Molecular Biology**

DISSERTATION

**Submitted to the University of New Hampshire
in Partial Fulfillment of
the Requirements for the Degree of**

**Doctor of Philosophy
in
Biochemistry**

May, 1999

UMI Number: 9926020

**UMI Microform 9926020
Copyright 1999, by UMI Company. All rights reserved.**

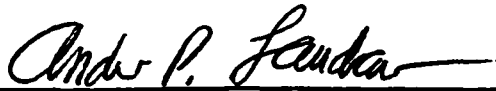
**This microform edition is protected against unauthorized
copying under Title 17, United States Code.**

UMI
300 North Zeeb Road
Ann Arbor, MI 48103

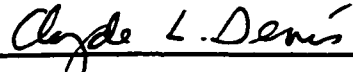
This dissertation has been examined and approved.



Dissertation Director, John J. Collins
Associate Professor of Biochemistry and
Molecular Biology



Andrew P. Laudano
Associate Professor of Biochemistry and
Molecular Biology



Clyde L. Denis
Professor of Biochemistry and Molecular
Biology



G. Eric Schaller
Assistant Professor of Biochemistry and
Molecular Biology



Charles W. Walker
Professor of Zoology

4/26/99

Date

DEDICATION

To my parents and my husband, Derek.

ACKNOWLEDGEMENTS

There are many people who have contributed to the work presented in this dissertation. Perhaps the greatest contributions have come from members of the lab - both past and present. Mindy Zhang, who initiated this project, was a great source of wisdom and advice during the time that she was in the lab. However, it is Queta Boese who has been my constant companion during the five years that I have spent at UNH. Queta has always provided advice and encouragement when it was needed. Perhaps more importantly, she has been someone to discuss my thoughts with - both scientific and personal.

As described within, characterization of the cellular phenotype and genetic analysis of *src-1(cj293)* mutants has been done in collaboration with Craig Mello's laboratory at the University of Massachusetts Medical Center in Worcester, Massachusetts. Yanxia Bei, a graduate student in Craig's lab, has significantly contributed to the story presented here. I am greatly indebted both to her and to Craig for taking such interest in furthering our understanding of the role SRC-1 plays in *C. elegans* development.

Lastly, the UNH faculty, especially my committee members John Collins, Andy Laudano, Clyde Denis, G. Eric Schaller, and Chuck Walker have provided guidance and support for my efforts. In particular, Andy has spent countless hours discussing experimental details with me and has provided encouragement and support on numerous occasions. As my advisor, John Collins has been a source of guidance, constructive comments, support, and encouragement during the five years that I have been part of his lab.

Thank you all for your help.

TABLE OF CONTENTS

DEDICATION	iii
ACKNOWLEDGEMENTS	iv
LIST OF TABLES	vii
LIST OF FIGURES	viii
ABSTRACT	x

	PAGE
INTRODUCTION	1
MATERIALS AND METHODS	6
Maintenance of <i>C. elegans</i> strains	6
Construction of <i>C. elegans</i> strains	7
Peptide synthesis and characterization	10
Antibody production	11
Antibody purification	12
Antibody characterization	13
Preparation of protein extracts	14
Immunoprecipitation	15
Western blot analysis	15
DNA Isolation	17
Polymerase chain reaction	17
DNA sequencing	19
Isolation of a <i>src-1</i> loss-of-function mutant	19
RNA isolation	21
Reverse transcription - PCR	21
Directed two-hybrid analysis	22

RESULTS	24
Analysis of SRC-1 phosphorylation	24
Mapping <i>src-1</i>	37
Isolation of a <i>src-1</i> deletion mutant	43
Molecular characterization of <i>src-1(cj293)</i>	44
Phenotypic characterization of <i>src-1(cj293)</i>	48
Testing for a direct interaction between SRC-1 and WRM-1	60
Testing for a genetic interaction between <i>src-1(cj293)</i> and <i>clr-1(e1745ts)</i>	64
DISCUSSION	66
<i>src-1</i> encodes a pp60 ^{c-src} ortholog	66
Maternal expression of <i>src-1</i> is essential, but zygotic expression is not	67
SRC-1 regulates morphogenesis and cell fate decisions of developing embryos .	70
Directed two-hybrid analysis fails to detect, but does not rule out, an interaction between SRC-1 and WRM-1	74
SRC-1 may be important for defining anterior-posterior polarity of asymmetric cell divisions	77
SRC-1 regulates cytoskeletal organization in concert with the MOM proteins, but does so independently of WRM-1 and POP-1	78
Mutation of the CLR-1 phosphatase is unable to suppress the Mel phenotype of <i>src-1</i> mutants	79
LIST OF REFERENCES	82
APPENDIX	89
Abbreviations	90
<i>C. elegans</i> gene names	91

LIST OF TABLES

	PAGE
Table 1: <i>C. elegans</i> strains	7
Table 2: Antibodies used for immunoprecipitation and western blotting	16
Table 3: PCR and sequencing primers	18
Table 4: <i>src-1(cj293)</i> maternal effect lethality	51
Table 5: Phenotypes of zygotically rescued <i>src-1(cj293)</i> heterozygotes	51
Table 6: Genetic analysis of intestine formation in <i>src-1</i> mutants	59
Table 7: Point mutations identified within the <i>src-1</i> insert of pTW44	62
Table 8: Genetic analysis of <i>src-1(cj293); clr-1(e1745ts)</i> double mutants	65

LIST OF FIGURES

		PAGE
Figure 1:	Predicted SRC-1 protein structure	25
Figure 2:	Alignment of SRC-1 and chicken pp60 ^{C-SRC} kinase domains	26
Figure 3:	Analysis of the phosphorylation state of wild-type SRC-1	28
Figure 4:	Mass spectrum analysis of phosphorylated SRC-1 peptide	29
Figure 5:	Sequence analysis of phosphorylated SRC-1 peptide	30
Figure 6:	Specificity of SRC-1 antibodies	36
Figure 7:	Strategy for following segregation of <i>src-1(cj290::Tc5)</i>	39
Figure 8:	<i>src-1(cj290::Tc5)</i> co-segregation frequencies	41
Figure 9:	PCR scoring of <i>src-1(cj290::Tc5)</i> co-segregation	42
Figure 10:	<i>src-1</i> deletion screen strategy	45
Figure 11:	Identification of <i>src-1(cj293)</i> as a PCR product	46
Figure 12:	Genomic structure of the deletion allele <i>src-1(cj293)</i>	47
Figure 13:	RT-PCR analysis of a <i>src-1(cj293)</i> transcript	49
Figure 14:	Proposed effect on <i>src-1(cj293)</i> protein if translated	50
Figure 15:	<i>src-1(cj293)</i> embryos exhibit defective morphogenesis	54
Figure 16:	Generation of <i>C. elegans</i> founder cells	55
Figure 17:	The <i>C. elegans</i> Mom pathway	57
Figure 18:	Genetic analysis of intestine formation in <i>src-1</i> mutants	58
Figure 19:	Two-hybrid assay to test for a SRC-1, WRM-1 interaction	61
Figure 20:	The Gal4p-SRC-1 fusion is expressed in yeast	63
Figure 21:	Alignment of <i>C. elegans</i> SRC-1 and F49B2.5 kinase domains	69
Figure 22:	Alignment of <i>C. elegans</i> SRC-1 and F49B2.5 SH2 domains	71

Figure 23:	A genetic model for SRC-1 function in regulating the intestinal cell fate decision	75
Figure 24:	A genetic model for the separable functions of SRC-1 and the MOM proteins in regulating spindle orientation and the intestinal cell fate decision	80

ABSTRACT

ISOLATION AND CHARACTERIZATION OF A *CAENORHABDITIS ELEGANS* SRC LOSS-OF-FUNCTION ALLELE USING REVERSE GENETICS.

by

Jennifer Dignan Hogan

University of New Hampshire, May, 1999

The vertebrate proto-oncogene Src is a protein-tyrosine kinase that has been implicated as a component of receptor-mediated signal transduction pathways important for cell growth and differentiation. Consistent with this notion, overexpression or activation of Src by mutation induces neoplastic transformation in cell culture, leads to tumorigenesis in laboratory animals, and has been observed in a number of human tumors. Despite years of intensive investigation, neither its role in oncogenesis nor its normal, biological role is understood.

To diminish the issue of redundancy that has complicated analysis of Src function in vertebrates and *Drosophila*, I have chosen to study Src function in the genetically less complex nematode *Caenorhabditis elegans*. The gene *src-1* encodes a protein with significant structural and sequence identity to vertebrate c-Src. The first part of this dissertation describes a set of biochemical experiments supporting the hypothesis that SRC-1 is the ortholog of vertebrate pp60^{c-src}. The second part of this dissertation describes the isolation and characterization of a *src-1* loss-of-function allele using a reverse genetic approach. *src-1(cj293)* is a deletion allele generated by *N*-ethyl-*N*-nitrosourea

mutagenesis that encodes a truncated, kinase-inactive protein. It is a recessive maternal effect lethal allele that interacts genetically with components of a conserved Wnt signaling pathway providing the first direct connection between two intensively studied vertebrate signaling pathways: Src and Wnt. The genetic interactions identified in combination with the embryonic defects observed in *src-1(cj293)* animals suggest that SRC-1 normally plays a role in regulating spindle orientation, morphogenesis, and cell fate decisions of developing *C. elegans* embryos. This study lays the ground work for additional genetic and biochemical analyses that will help define the molecular details of SRC-1 signaling. Such experiments will shed light not only on the biological role SRC-1 plays in *C. elegans* development, but also the biological role of Src-family kinases in general. Ultimately, these analyses may provide insight into the mode of action of oncogenic Src mutants.

INTRODUCTION

Src is the prototype member of a family of membrane-associated protein-tyrosine kinases that transduce signals from cell surface receptors to downstream targets in response to a diverse array of stimuli. Src kinase activity is normally tightly regulated by reversible phosphorylation. Loss of regulation, seen in both tumor virus encoded v-Src and activated forms of its cellular counterpart c-Src, induces neoplastic transformation in cell culture and leads to tumorigenesis in laboratory animals. Overexpression or activation of Src has been reported in a number of human tumors including primary breast carcinoma (Verbeek et al., 1996) and colorectal cancer (Cartwright et al., 1994; Talamonti et al., 1993). Cumulatively, these observations suggest that Src has an important role in cell proliferation, but neither its role in oncogenesis nor its normal, biological role is understood.

Most of our knowledge about Src function is the result of biochemical experiments conducted with vertebrate cell lines. Upstream activators of Src include a number of growth factor receptors. In particular, the ligand-dependent activation of Src by the platelet-derived growth factor (PDGF) receptor has been well characterized (Gould and Hunter, 1988; Ferrell and Martin, 1989; Kypta et al., 1990). When activated, Src appears to mediate its effects by signaling through Ras (Mulcahy et al., 1985; Smith et al., 1986), MAP-kinase (Gupta et al., 1992) and PI-3-kinase (Fukui et al., 1991) pathways. To explore the role that Src plays in these signaling pathways, studies have been conducted to identify its downstream targets. These putative targets of Src signaling fall into diverse functional categories. Some recent examples include: focal adhesion proteins FAK (Cobb et al., 1994; Schaller et al., 1994) and paxillin (Weng et al., 1993); cortactin, a cytoskeletal protein (Wu et al., 1991); Stat3, a transcription factor (Cao et al., 1996); and Sam68, an RNA-binding protein involved in mitosis (Fumagalli et al., 1994; Taylor and Shalloway, 1994). Unfortunately, the presence of multiple, closely related tyrosine kinases has made it

difficult to identify which, if any, are the biologically relevant targets.

Genetic analysis of Src function in mice highlights the complexity of these issues. Src knock-out mice are viable and develop normally except for a bone modeling disorder, osteopetrosis (Soriano et al., 1991). This surprisingly mild phenotype has been attributed to genetic redundancy with closely related tyrosine kinases. Consistent with this theory, mice lacking Fyn or c-Yes, the other ubiquitously expressed Src-family members, exhibit similarly restrictive phenotypes (Stein et al., 1992; Appleby et al., 1992; Grant et al., 1992; Stein et al., 1994). As would be expected, *src; fyn* and *src; yes* double mutant mice exhibit more severe defects, dying shortly after birth, and *src; fyn; yes* triple mutants die *in utero* (Stein et al., 1994).

The *c-src* gene has been identified in a wide variety of organisms other than vertebrates including hydra, sponge, *Xenopus*, and *Drosophila*. The overall structure and sequence of the c-Src protein is well conserved through evolution suggesting that these distantly related proteins likely share conserved functions with vertebrate c-Src. Therefore, it should be possible to investigate the function of c-Src in model organisms like *Caenorhabditis elegans*. Properties of this small, free living nematode that make it ideal for genetic analysis include the fact that it is easy to cultivate in the laboratory, has a short generation time of less than four days, and has a large brood size. Individuals reproduce as self-fertile hermaphrodites, but males arise naturally at a low frequency making genetic crosses possible. Analysis of mutants is made easy by the fact that development of this organism is well characterized. Its complete, invariant cell lineage is known and any alteration during development can be resolved at the level of individual cells since the body of the nematode is transparent. Recent completion of the *C. elegans* genome sequence permits the rapid identification of homologs to interesting vertebrate or *Drosophila* genes. Established reverse genetic approaches make isolating mutant alleles of these genes routine. Once a mutant has been isolated, it can be subjected to the powerful genetic methods available in this organism in order to elucidate the role that the gene of interest plays in *C. elegans* development.

C. elegans development is unique in that it follows an invariant cell lineage to

generate (at hatching) an organism of 558 cells that are all derived from five somatic founder cells: AB, C, D, E, and MS. These founder cells are formed by a series of asymmetric and asynchronous cell divisions following fertilization. Each gives rise to a unique and diverse set of cell fates. Despite the apparent simplicity implied by invariance, generation of the founder cells has been shown to depend both on asymmetric segregation of cell-fate determinants and intracellular signaling (reviewed in Rose and Kemphues, 1998). At least three cell-signaling pathways have been shown to be important for establishing founder cell fates. The six *par* genes are important for generating asymmetry along the anterior-posterior axis of one-cell stage embryos (reviewed in Guo and Kemphues, 1996). More recently, the highly conserved Wnt / Wg signaling pathway has been shown to be important for generating asymmetry along the anterior-posterior axis of the EMS blastomere of four-cell stage embryos (Rocheleau et al., 1997; Thorpe et al., 1997). This pathway has been the subject of intense investigation in both *Drosophila* and mice which require it for normal development. In *C. elegans*, MOM-2 signal is believed to be secreted from the P2 blastomere (Rocheleau et al., 1997; Thorpe et al., 1997). This signal presumably binds the MOM-5 receptor located on the surface of the adjacent EMS blastomere activating the signaling pathway within this cell. The signal is propagated through WRM-1 culminating in decreased levels of the presumed transcription factor POP-1 which results in specification of the E founder cell fate. The third pathway is defined by *lit-1*, an as yet unidentified gene that is important for establishing anterior-posterior polarity throughout all embryonic cell lineages (Kaletta et al., 1997). Disruption of any of these signaling pathways leads to characteristic defects in cell fate decisions that can be visualized at the level of individual cells.

Studies of postembryonic *C. elegans* vulval development and dauer formation have revealed the evolutionary conservation of two other cell-signaling pathways: the ras/MAP-kinase (Sundaram and Han, 1996) and PI-3-kinase (Thomas and Inoue, 1998) pathways. Formation of the vulva is directed by LIN-3 signaling (reviewed in Sundaram and Han, 1996). LIN-3, an epidermal growth factor (EGF)-related protein binds to the *C. elegans* EGF receptor homolog LET-23 . Activation of LET-23 recruits SEM-5 (Grb2), LET-60

(Ras), and LIN-45 (Raf) which transduces the signal through the MAP-kinase pathway to stimulate differentiation of vulval precursor cells. Migration of sex myoblasts (muscles important for egg laying), which is partially directed by EGL-17 (FGF) signaling (Burdine et al., 1997), also appears to be dependent upon the MAP-kinase pathway (Sundaram et al., 1996).

The dauer larvae is a modified third larval stage that is induced by stressful environmental conditions. Individuals can live for several months before exiting from the dauer state at which time they resume their normal life cycle. Presumably, this larval stage has been adapted as a mechanism by which to survive harsh conditions. Non-dauer development has recently been shown to be directed by signaling through DAF-2, an insulin receptor-like tyrosine kinase (Kimura et al., 1997). Phosphorylation of DAF-2 is predicted to recruit an as yet unidentified p85 subunit of PI-3-K which activates AGE-1, the p110 subunit of PI-3-K (Morris et al., 1996). AGE-1 converts phosphatidylinositol to the second messenger phosphatidylinositol-3,4,5-triphosphate which appears to promote non-dauer development, accelerate aging, and reduce fat and glycogen storage (reviewed in Thomas and Inoue, 1998). Conservation of this PI-3-kinase signaling pathway and the ras/MAP-kinase pathway suggests that the function of SRC-1, and its role in these pathways will also be conserved. At the same time, the less complex nematode genome contains fewer Src-related genes thereby diminishing the issue of redundancy that has complicated genetic analysis of Src function in mice and most recently has complicated genetic analysis of Src function in *Drosophila*.

src-1, a *C. elegans c-src* homolog, was cloned by screening a mixed stage cDNA library with a probe derived from *v-src*, the viral oncogene encoded by the Rous sarcoma virus (Thacker and Capecchi, personal communication). The predicted protein encoded by this gene contains extensive structural and amino acid similarity to the vertebrate Src protein. The first goal of my dissertation project has been to determine if the SRC-1 protein is regulated by reversible tyrosine phosphorylation in the same manner as vertebrate pp60^{c-src}. Specifically, my goal was to determine whether the nematode protein is normally found in a state of phosphorylation associated with the kinase active form of

pp60^{c-src}. To address this issue, I have developed an antibody which specifically recognizes the tyrosine 416 phosphorylated form of SRC-1. Immunoprecipitation and western blotting experiments performed with this antibody suggest that some fraction of SRC-1 is normally phosphorylated at this tyrosine residue as would be expected for a Src-related kinase.

The second goal of my dissertation project has been to gain insight into the role that SRC-1 plays in *C. elegans* development. Overexpression studies of both wild-type and unregulated (Y527F) SRC-1 have suggested that the protein may indeed act on the conserved ras/MAP-kinase signaling pathway initiated by EGL-17 signal (Thacker and Capecchi, personal communication). To better understand its role in this and other developmentally important pathways, it will be important to subject *src-1* to genetic analysis. Such analysis requires a *src-1* mutant allele which I have isolated using a PCR-based reverse genetic approach. Phenotypic characterization has determined that this loss-of-function *src-1* allele is maternal effect lethal, identifying, for the first time, an essential role for a Src-family kinase. Using information gained from characterization of the mutant phenotype, I have begun to address which signaling pathways SRC-1 may normally act upon during *C. elegans* development. Genetic analysis of the *src-1* mutant allele has suggested that SRC-1 may act on a conserved Wnt pathway to regulate spindle orientation, morphogenesis, and cell fate decisions of developing embryos.

MATERIALS AND METHODS

Maintenance of *C. elegans* Strains

Table 1 contains a list of strains used in the experiments described. All strains, except CB3241, were grown at 20°C on Nematode Growth Media (NGM: 17g Agar, 2.5g Peptone per liter, and 50mM NaCl, 25mM KHPO₄ pH 6.0, 1mM CaCl₂, 1mM MgSO₄, 5µg/ml cholesterol) or in liquid cultures of S medium (S med: 0.1M NaCl, 50mM KHPO₄ pH 6, 10mM K-Citrate pH 6, 3mM CaCl₂, 3mM MgSO₄, 5µg/ml cholesterol, trace metals). CB3241 was maintained at the permissible temperature of 16°C and shifted to the restrictive temperature of 25°C as necessary. *Escherichia coli* strains OP50 and RR1 were used as food sources.

Table 1 - *C. elegans* strains.

Strain	Genotype	Source
AF1	<i>+/szT1[lon-2(e678)]I;</i> <i>dpy-8(e1321)unc-3(e151)/szT1 X</i>	CGC
BE108	<i>sqt-2(sc108)</i>	CGC
CB12	<i>dpy-9(e12)</i>	CGC
CB128	<i>dpy-10(e128)</i>	CGC
CB224	<i>dpy-11(e224)</i>	CGC
CB315	<i>unc-34(e315)</i>	CGC
CB369	<i>unc-51(e369)</i>	CGC
CB444	<i>unc52(e444)</i>	CGC
CB518	<i>bli-5(e518)</i>	CGC
CB767	<i>bli-3(e767)</i>	CGC
CB1166	<i>dpy-4(e1166)</i>	CGC
CB3241	<i>clr-1(e1745ts)</i>	M. Stern
KR16	<i>unc-11(e47) dpy-5(e61); sDp2(I:f)</i>	CGC
N2	<i>wild type (Bristol)</i>	P. Anderson
SP1697	<i>dpy-1(e1) ncl-1(e1865) unc-36(e251)</i>	V. Ambros
TR1034	<i>unc-22(r644::Tc5) mut-2(r459)</i>	P. Anderson
TR1299	<i>unc-54(r323::Tc1)</i>	P. Anderson
TW195	<i>dpy-5(e61)</i>	-----
TW400	<i>src-1(cj290::Tc5)</i>	-----
TW410	<i>mut-2(r459) sem-4(n1378)</i>	-----
TW411	<i>src-1(cj290::Tc5) mut-2(r459) sem-4(n1378)</i>	-----
TW412	<i>src-1(cj293); bli-3 / src-1; bli-3(e767)</i>	-----
TW416	<i>src-1(cj293) / szT1[lon-2(e678)] I;</i> <i>dpy-8(e1321) unc-3(e151) / szT1 X</i>	-----
TW424	<i>src-1(cj293); sDp2(I:f)</i>	-----
TW425	<i>clr-1(e1745ts); src-1(cj293) / src-1(cj293),</i> <i>src-1(cj293) / +, or + / +</i>	-----

Construction of *C. elegans* Strains.

Mapping strains. Fifteen strains were constructed to test for linkage of *src-1* with genetic markers on the left, middle, and right arm of each of the five autosomes. Males

heterozygous for the genetic marker of choice were mated to TW400 hermaphrodites. F1 individuals were picked singly. Those that segregated F2 progeny homozygous for the chosen marker were retained. The homozygous F2 progeny were subsequently assayed individually for co-segregation of *src-1(cj290::Tc5)* by PCR.

Strain TW411. The purpose of this construction was to place *src-1(cj290::Tc5)* into a *mut-2(r459)* background which permits excision of Tc5. Males heterozygous for *mut-2(r459)* and the linked marker *sem-4(n1378)* were crossed to TW400 hermaphrodites. F2 Sem progeny were presumed to also be homozygous for *mut-2(r459)*. These animals were picked singly to fresh NGM plates. When the F3 generation began to emerge, DNA was isolated from the F2 Sem parents and PCR was performed to determine their genotype at the *src-1* locus. The populations established by individuals determined to be homozygous for *src-1(cj290::Tc5)* were subsequently subjected to additional PCR analysis in order to confirm that only the transposon-tagged allele of *src-1* was present. These populations were further screened for the presence of a high incidence of males (Him) phenotype that is associated with *mut-2(r459)*. One population meeting this criteria was selected to represent strain TW411.

Strain TW416. The purpose of this construction was to balance the *src-1(cj293)* allele so that it could be maintained in a heterozygous state without the concern of losing the allele through recombination with its sister chromatid. Strain AF1 bears the translocation *szT1(I;X)* which suppresses recombination events on the left arm of linkage group I. This strain spontaneously segregates males that have a distinct long (Lon) phenotype and are hemizygous for the translocation (Fodor and Deak, 1982). The Lon males were mated to *src-1(cj293)* homozygous hermaphrodites identified by virtue of the linked Ske phenotype. Due to partial zygotic rescue by the wild-type *src-1* allele supplied by the Lon males, a small fraction of embryos hatch. All wild-type hermaphrodite progeny resulting from the cross must be heterozygous for both *szT1(I;X)* and *src-1(cj293)*. These individuals segregate wild-type heterozygotes, arrested aneuploid embryos, hermaphrodites that are both Ske and Mel, and Lon males. The strain is maintained by picking wild-type

individuals.

Strain TW424. The purpose of this construction was to balance the *src-1(cj293)* allele so that it could be maintained in a homozygous state. Strain KR16 bears the free duplication *sDp2(I;f)*. This duplication covers the left arm of linkage group I rescuing the dumpy (Dpy) and uncoordinated (Unc) phenotype characteristic of the *unc-11(e47); dpy-5(e61)* background of this strain. Animals that have lost the duplication are readily identified as DpyUncs. Since *sDp2(I;f)* is not transmitted by males (Rose et al., 1984), wild-type KR16 hermaphrodites were mated by males heterozygous for *src-1(cj293)*. F1 hermaphrodites were picked singly. Those that segregated a low frequency of DpyUnc animals (instead of 25% DpyUnc) were presumed to have retained the duplication. The lines that also segregated *src-1(cj293)* homozygotes (identified by virtue of the linked Ske phenotype) were chosen for further analysis. Wild-type F2 animals from these lines were picked singly. Those animals bearing *sDp2(I;f)* in a *src-1(cj293)* homozygous background were identified by their unique ability to segregate F3 progeny that, while mostly wild type, were occasionally Ske and Mel but were never DpyUnc. One line meeting this criteria was selected to represent strain TW424.

Strain TW425. The purpose of this construction was to build a *src-1(cj293); clr-1(e1745ts)* double mutant in order to test for a genetic interaction between the two genes. Males heterozygous for *clr-1(e1745ts)* were mated to *src-1(cj293)* homozygous hermaphrodites identified by virtue of the linked Ske phenotype. Due to partial zygotic rescue by the wild-type *src-1* allele supplied by the males, a small fraction of embryos hatch. These F1 individuals were picked singly. As the F2 generation matured, ten individuals were randomly picked from each population and shifted to 25°C overnight. At this restrictive temperature, *clr-1(e1745ts)* homozygotes are readily identifiable by their clear (Clr) phenotype. Those populations that produced Clr animals must have been established with an F1 individual heterozygous for both *src-1(cj293)* and *clr-1(e1745ts)*. Apparently wild-type individuals from the remaining, unshifted progeny were picked singly. After, the F3 generation had emerged, the F2 parents were shifted to 25°C. Those

that exhibited the Clr phenotype were presumed to have established a population homozygous for *clr-1(e1745)*. These F3 populations were screened for segregation of *src-1(cj293)* homozygotes identified by virtue of the linked Ske phenotype. One such population was chosen to represent strain TW425. This strain is maintained at the permissive temperature (16°C) by picking apparently wild-type worms that segregate individuals that are both Ske and Mel.

Peptide Synthesis and Characterization

Phosphorylated and nonphosphorylated 15mer peptides were modeled on the predicted amino acid sequence surrounding tyrosine 416 of the *C. elegans* SRC-1 protein. The sequence of these peptides is Lys-Leu-Met-Glu-Glu-Asp-Ile-(Tyr or P-Tyr)-Glu-Ala-Arg-Thr-Gly-Ala-Lys. Both peptides were synthesized using Fast Moc™ chemistry on an Applied Biosystems Model 431A peptide synthesizer equipped with version 1.12 software.

Cleavage of peptides from the resin. The cleavage procedure used to isolate the peptides from the resin was recommended by Ruth Steinbrich of Applied Biosystems / Perkin Elmer (Steinbrich, 1993). The cleavage mixture contained 0.75g crystalline phenol, 0.25ml EDT, 0.5ml thioanisole, 0.5ml distilled water, and 10ml TFA. The cleavage mixture was cooled on ice, added to the peptide-resin, and allowed to incubate at room temperature for 90 minutes.

The cleaved peptides were precipitated by vacuum filtration into 200ml of ice-cold methyl t-butyl ether (MtBE) and washed three times with additional MtBE. After the final wash, the peptides were resuspended in 50% acetic acid and lyophilized overnight. Both were lyophilized once more from distilled water and stored at -20°C.

Desalting the cleaved peptides. The peptides were desalted on G-15 Sephadex equilibrated in 50% acetic acid. Collected fractions were analyzed for the presence of the peptides using a ninhydrin test. A 10µl aliquot of each fraction was spotted on Whatman paper, dried, dipped in a 1% ninhydrin acetone solution, and baked at 90°C for five

minutes. Ninhydrin reacts with the amino group of peptides to form a purple color that was used to identify the peptide containing fractions. The peptides were then lyophilized from the 50% acetic acid solution overnight. Both were lyophilized once more from distilled water and stored at -20°C.

Molecular weight and sequence analysis. The molecular weight of each peptide was confirmed by mass spectrum analysis performed by Mass Search Company. In both cases, the confirmed molecular weight matched the predicted molecular weight with a difference of less than two daltons. The sequence of the phosphorylated peptide was confirmed by the Edman degradation method of N-terminal analysis using a Porton Instruments Model 2090 automated sequencer.

Antibody Production

Coupling the phosphorylated 15mer peptide to BSA. The phosphorylated peptide was coupled to bovine serum albumin (BSA) separately with glutaraldehyde and NHS and EDC. For the glutaraldehyde coupling, 13mg of peptide (a 35-fold molar excess) was dissolved in 0.5ml of distilled water and adjusted to pH 7.0. A 13mg sample of BSA was dissolved in 0.5ml of 0.2M NaHPO₄, pH 7.5. The peptide and BSA solutions were combined and 0.5ml of 0.02M glutaraldehyde was added drop wise while vortexing. The solution was mixed end-over-end at room temperature for 30 minutes then dialyzed versus 4L of phosphate buffered saline (PBS: 0.14M NaCl, 2.7mM KCl, 8mM Na₂HPO₄, and 1.5mM KH₂PO₄) which was changed two times during the two day dialysis period at 4°C.

For the NHS and EDC coupling, 15mg of peptide (a 30-fold molar excess) was dissolved in 1ml of distilled water and adjusted to pH 7.0. To give a final concentration of 0.1M NaHCO₃, 1ml of 0.2M NaHCO₃ was added to the peptide solution. A 15ml aliquot of column-purified acetylated BSA (approximately 6mg/ml) was combined with 200mg EDC and stirred at room temperature for five minutes. A 250mg sample of NHS was added to the BSA solution and stirred at room temperature for 15 minutes. This activated BSA solution was gel filtered through a Sephadex G-50 column equilibrated with PBS at

4°C. 10ml (approximately 18mg) of filtered, activated BSA was combined with the peptide solution and stirred overnight at 4°C. The solution was dialyzed versus PBS for two days at 4°C. The coupled peptides were stored at -20°C.

Antisera Production. Three New Zealand white rabbits (961, 962, 963) were immunized for antisera collection. A 1mg/ml solution containing a 1:1 ratio of NHS and EDC-coupled peptide to glutaraldehyde-coupled peptide was used for the injections. All injections were done subcutaneously. For the first injection, 4ml of the 1mg/ml peptide solution was emulsified with 2ml of complete Freund's adjuvant and 2ml of incomplete Freund's adjuvant. For subsequent injections, 4ml of the 1mg/ml peptide solution was emulsified with 4ml of incomplete Freund's adjuvant. The rabbits were boosted a total of six times at approximately two week intervals.

Antibody Purification.

Antibodies recognizing the phosphorylated SRC-1 peptide were purified from sera collected from rabbit #961 using affinity chromatography.

Coupling peptides to CNBr-activated sepharose. Phosphotyrosine, nonphosphorylated peptide, and phosphorylated peptide were individually coupled to cyanogen bromide (CNBr)-activated Sepharose 4B using the following protocol. Approximately 1 μ mol of ligand per ml of gel was dissolved in coupling buffer (0.1M NaHCO₃, 0.5M NaCl; pH 8.3) and the pH was adjusted to 8.0. Immediately prior to addition of the ligand solution, the gel (previously swollen and washed with 1mM HCl) was quickly washed with coupling buffer. The ligand and gel mixture (at a 2:1 ratio) was allowed to rotate end-over-end overnight at 4°C. The following day, the excess ligand was washed away with coupling buffer and 1M ethanolamine (pH 8.0) was added to block excess reactive groups. This solution was allowed to rotate end-over-end for two hours at room temperature (or overnight at 4°C). The coupled gel was subsequently washed with four to five cycles of alternating high (0.1M NaHCO₃, 0.5M NaCl; pH 8.3) and low

(0.1M NaOAc, 0.5M NaCl; pH 4.0) pH buffers to removed any non-covalently bound compounds. The coupled gel was finally washed with 1M NaCl before storing at 4°C.

Purification of immune sera. Immune sera from rabbit #961 (bled on 5/31/96) was purified by affinity chromatography. A series of agarose / sepharose columns were set up using syringe barrels lined with glass wool and attached to stop cocks. Three negative selection columns were used: BSA-agarose (Sigma) (5ml), phosphotyrosine-sepharose (5ml), and non-phosphorylated SRC-1 15mer-sepharose (3ml). The purpose of these columns was to deplete any cross reacting antibodies contained in the sera. The fourth column, phosphorylated SRC-1 15mer-sepharose (1ml), was the positive selection column which served to specifically isolate the desired antibodies from the sera. After equilibrating with PBS, 5ml of immune sera was added to the series of columns. After the sera had passed though each of the four columns, the positive selection column was separated from the series of columns and washed with 50 volumes of PBS. The column was next washed with 10 volumes of 1M NaCl to remove any weakly bound compounds. Following this wash, the antibodies were eluted sequentially with 3.5M MgCl₂ and 4.5M MgCl₂. A total of seven fractions were collected containing about 3ml of eluent each. All fractions were immediately dialyzed at 4°C versus 4L of PBS which was changed twice during the two day dialysis period. All dialyzed fractions were subsequently stored at -20°C.

Antibody Characterization.

An indirect enzyme-linked immunosorbent assay (ELISA) was used to characterize the specificity of each purified fraction. Ninety six well plates coated with 100µl of 0.2M carbonate-bicarbonate buffer containing 10µg/ml antigen were incubated overnight at room temperature. Plates were rinsed three times with PBS (0.5%) Tween-20 (PBST) then incubated with PBS (0.1%) ovalbumin for one hour at room temperature to block non-specific binding. 100µl of affinity-purified sera (at varying dilutions) were added to each well after emptying of blocking buffer. Plates were incubated for one hour at room temperature then rinsed three times with PBST before addition of 100µl Donkey anti-rabbit

polyclonal antibody (1:2000) conjugated to horseradish peroxidase (HRP). Plates were incubated for two hours then rinsed three times with PBST. A fourth wash was allowed to incubate for five minutes. Sigma Fast solution (one urea tablet plus one o-phenylene diamine tablet per 20ml distilled water) (Sigma) was freshly prepared and 100 μ l was added to each well. Up to 30 minutes was allowed for color production before the plates were read on a Bio-Tek instruments microplate autoreader at 405nm. Fraction #1 demonstrated the best profile, therefore, it was used for all subsequent analyses.

Preparation of Protein Extracts.

C. elegans protein extracts. Worms were harvested from liquid culture by centrifugation. After rinsing two to three times with distilled water, the worms were further cleaned using a 35% sucrose gradient. Following an additional distilled water wash, they were suspended in ice-cold extraction buffer (250mM sucrose, 10mM Tris-HCl pH 8.0, 10mM MgCl₂, 1mM EGTA; added immediately before use: 1mM sodium orthovanadate; 0.025 mg/ml aprotinin; 0.01 mg/ml pepstatin; 1mM PMSF; 0.5 mM DTT; 10mM benzamidine) at a ratio of 1:1 and were ground in liquid nitrogen with a mortar and pestle. Samples were stored at -80°C until needed. At such time the ground worms were allowed to thaw at 4°C (all subsequent manipulations were carried out at 4°C). During this time an additional volume of extraction buffer (containing all phosphatase and protease inhibitors) was added to the samples. Once the ground worms had completely thawed, 10% NP40 was added to a final concentration of 1% NP40 to disrupt intact membranes. Samples were centrifuged at 12,000 rpm for five minutes. The supernatant was precleared as previously described (Laudano and Buchanan, 1986) to reduce non-specific binding before being used for immunoprecipitation.

Yeast protein extracts. Overnight cultures (5ml) were pelleted and washed with distilled water before resuspending in 250 μ l SDS harvest buffer (10mM Tris-HCl pH 7.4, 1mM EDTA, 0.5% SDS, 0.025mg/ml aprotinin, 1mM PMSF, 0.5mM DTT) on ice. After the addition of 250mg of glass beads (Sigma), the samples were vortexed for two minutes

followed by boiling for five minutes. The supernatant was isolated by centrifugation at 4°C and 10% NP40 was added to a final concentration of 1% NP40 to attenuate excess SDS. After adding an equal volume of 2X SDS sample buffer containing 10% 2-mercaptoethanol, the samples were boiled for five minutes. All protein extracts were stored at -80°C until analyzed by SDS-PAGE followed by western blotting. Extracts used for immunoprecipitation were prepared in the same manner except that they were not boiled in SDS sample buffer prior to use.

Immunoprecipitation.

Prior to the addition of precleared protein extracts, 20µl of antibody was preincubated on ice with an equal volume of 10mM blocking peptide (pH 7.0) for 15 minutes when appropriate. Blocking peptides used included nonphosphorylated SRC-1 15mer, phosphorylated SRC-1 15mer, phosphorylated c-Src 15mer, and the free amino acid phosphotyrosine. An equivalent amount of distilled water was added to samples not subject to any peptide block to maintain equal volumes. Precleared protein extracts, 0.2-1ml, were added to the antibody solutions and incubated on ice with occasional mixing for 60-90 minutes. Immune complexes were precipitated by incubating samples with 20µl of protein A agarose (Pharmacia) for 60-90 minutes under the same conditions. Samples were washed five times with extraction buffer (no protease inhibitors) containing 1% NP40 to remove non-specifically bound proteins. To elute bound proteins from the protein A agarose, samples were boiled for five minutes in 20µl of 2X SDS sample buffer (62.5mM Tris-HCl, 2.3% SDS, 0.1% bromophenol blue, 10% glycerol) containing 10% 2-mercaptoethanol. All samples were stored at -80°C.

Western Blot Analysis.

SDS gel electrophoresis. Samples were analyzed by SDS-PAGE in a discontinuous 1.5mm slab gel system essentially as described by Laemmli (1970). Buffers

and solutions for the preparation and running of the gel were prepared as described by O'Farrel (1975). Depending on the experiment, either a nine or twelve percent running gel was used. Sigma Prestained Standards (β -galactosidase, 116,000; fructose-6-phosphate kinase, 84,000; pyruvate kinase, 58,000; ovalbumin, 45,000; lactic dehydrogenase, 36,500; triosephosphate isomerase, 26,600) were used to estimate the molecular weight of resolved proteins.

Western blotting. Once separated by SDS-PAGE, proteins were electrophoretically transferred to a nitrocellulose membrane. To block non-specific binding, the membrane was incubated in PBS (0.1%) Tween-20 (PBST) containing 10% dry milk for 60 minutes. After quickly rinsing the membrane with PBST, it was subjected to an additional 15 minute wash and two 5 minute washes. The primary antibody, diluted 1:5000 in PBST containing 10% dry milk, was incubated with the membrane for 60 minutes. This incubation was followed by a series of washes before addition of the secondary (HRP-conjugated) antibody also diluted 1:5000 in PBST containing 10% dry milk. After a 60 minute incubation, the membrane was washed before using enhanced chemiluminescent (ECL) detection (Amersham) to develop the blot. Antibodies used in the experiments described are listed in Table 2.

Table 2 - Antibodies used for immunoprecipitation and western blotting.

Antibody	Source
anti-HA	Santa Cruz
anti-phosphotyrosine (4G10)	Upstate Biotechnology
anti-SRC-1	C. Thacker
anti-PY416SRC-1	-----
donkey anti-rabbit IgG - HRP	Amersham
sheep anti-mouse IgG - HRP	Amersham

DNA Isolation.

Worms were washed from NGM plates with M9 buffer (42mM Na₂HPO₄, 22mM KH₂PO₄, 8.5mM NaCl, 1mM MgSO₄) and rinsed with distilled water. Worms were suspended in 100µl of Worm Lysis Buffer (WLB: 50mM KCl, 10mM Tris-HCl pH 8.2, 2.5mM MgCl₂, 0.45% Tween-20, 0.45% NP40, 0.01% gelatin) and incubated in a dry ice / ethanol bath for 15 minutes. For enzymatic degradation, 2µl of 10mg/ml Proteinase K was added and the samples were incubated for one hour at 65°C. The enzyme was inactivated by incubation at 95°C for 15 minutes. The same protocol was followed for isolation of DNA from single worms except that individual worms were picked directly to 25µl of WLB and only 0.5µl of proteinase K was added for enzymatic degradation. All DNA template preparations were stored at -20°C.

Polymerase Chain Reaction.

A typical 25µl reaction contained the following:

0.5µl 50X buffer (20mM Tris-HCl pH 8.0, 250nM EDTA)
2.5µl 10X buffer (100mM Tris-HCl pH 8.8, 15mM MgCl₂, 250mM KCl)
0.1µl 100mM dNTPs
0.25µl 100pmol/µl primer #1
0.25µl 100pmol/µl primer #2
0.25µl Taq DNA Polymerase
16.15-20.15µl distilled water

Reactions were overlaid with 25µl mineral oil.

1-5µl DNA template

Table 3 lists all primers used. Reactions were placed in a thermal cycler. A typical profile consisted of 30 cycles at 94°C for 40 seconds, 54°C for 60 seconds, and 72°C for 60 seconds, followed by a final extension at 72°C for 10 minutes. The annealing temperature and extension time was adjusted as needed for individual reactions. All reactions were resolved by electrophoresis on a 0.8% SeaKem LE (FMC) agarose gel in 1X TAE (40mM Tris, 20mM acetic acid, 1mM EDTA pH 8.0). Lambda DNA (Promega) digested with HindIII was used as a marker to estimate the size of resolved DNA fragments.

Table 3 - PCR and sequencing primers.

Primer	Sequence 5' → 3'	Location
JC13	TTCATGTTGGAGCCAAGTCA	<i>unc-22</i>
JC14	TCGCAAGTGAACACGGCTCT	<i>unc-22</i>
JC41	TATACTCGAGAATTCTAC(T) ₁₈ V	oligodT
JC42	TATACTCGAGAATTCTAC	"anchor"
JC59	AACACTACAAAATCAAACGACTGG	<i>src-1</i> , exon 5
JC60	GTCAACTTACATTCCCAGCACCTC	<i>src-1</i> , exon 5
JC61	TCGTGCCTCGTAAATGTCCTCTTC	<i>src-1</i> , exon 6
JC62	CCTGTCCCTTTGTCATAATCTCAT	<i>src-1</i> , exon 6
JC71	CGAAACTCACGCCACTACCACT	Tc5
JC76	AAGCTTGAAATCGCGAATGTTAT	<i>src-1</i> , intron 5
JC90	GGTGGAGTACCACGAAATCTGG	<i>src-1</i> , intron 5
JC98	ACGCCCCAACAACAGACAGTATT	<i>src-1</i> , exon 3
JC99	ACTCTGGTCGCCCTCTATCC	<i>src-1</i> , exon 3
JC112	TACGCAGGAAAGATACCAAGAAAT	<i>src-1</i> , exon 4
JC113	ATACCGATGATCAGAGAAATGG	<i>src-1</i> , exon 4
JC125	ATTCCGCGCCATTTCCATA	<i>src-1</i> , exon 5
JC155	AATTCCTCGGCACATAACCAGTCT	<i>src-1</i> , exon 3
JC156	AAGCCCAAATAATGAAGCAATGTG	<i>src-1</i> , exon 6
JC194	CATGCCATGGGTTGCCTGTTTTCA	<i>src-1</i> , exon 2
JC195	GCCGCTCGAGGCACTTGGTGGCGC	<i>src-1</i> , exon 7
JC199	GCGCGGGATCCGAATGCACAATCGTG	<i>src-1</i> , exon 7
JC200	ATATACGCGGCCGCGCACTTGGTGG	<i>src-1</i> , exon 7
JC201	TATATGCGGCCGCGTAAAAAATTGTG	<i>src-1</i> , exon 7
JC202	CGCGCCTCTAGGAAAAGGCATTGAAA	<i>src-1</i> , exon 7

DNA Sequencing.

PCR products. PCR products were purified for sequencing by running the reaction on a 1% NuSieve GTG (FMC) agarose gel. The DNA was extracted from the gel using a Qiagen Gel Extraction kit according to manufacturer guidelines. Approximately 50ng of DNA was submitted to the DNA Sequencing Facility in the laboratory of Dr. Kocher, Department of Zoology, University of New Hampshire to be sequenced on an ABI automatic DNA sequencer.

Plasmids. Plasmids were purified directly from bacteria using a Promega Miniprep kit according to manufacturer guidelines. Approximately 250ng of DNA was submitted to the DNA Sequencing Facility.

Isolation of a *src-1* Loss-of-Function Mutant.

The chemical mutagen ENU was used to generate a deletion within the *src-1* gene. This mutation, designated *cj293*, was identified in a complex wild-type background using a PCR-based screen. Once identified, the *cj293* allele was isolated from the wild-type background using a process of subdivision and enrichment that is termed sib selection.

ENU mutagenesis. Synchronized, L4 stage hermaphrodites of the wild-type strain N2 were washed off NGM plates with M9 buffer. The worms were pelleted by centrifugation and resuspended in 4ml of M9 buffer containing 1mM *N*-ethyl-*N*-nitrosourea (ENU). After shaking in this solution for four hours at 20°C, the worms were washed three times with M9 buffer and then transferred to fresh NGM plates and allowed to lay eggs overnight. The following day, the embryos were harvested by washing the worms off the NGM plates with a dilute bleach solution (0.2M NaOH, 60% M9 buffer, 38% bleach). This solution degrades the cuticle and kills all worms, but is impermeable to the chitinous shell that surrounds embryos thereby isolating the embryos away from individuals of all other stages. The embryos were collected by centrifugation and washed

with M9 buffer before being allowed to hatch in M9 buffer on a rotary shaker incubated at 20°C overnight. In the absence of food, the hatched L1 larvae starve and enter the alternative dauer stage. The following day, the dauer larvae were collected by centrifugation and aliquotted to NGM plates with approximately 200 worms per plate (this represents the F1 generation). When introduced to food the larvae leave the dauer stage and progress through development normally. Because all larvae were introduced to food at the same time, they will develop in synchrony.

When the F2 generation had emerged, the plates (each representing one mutagenized population) were prepared for PCR analysis. Worms were washed off each plate with M9 buffer and divided into three portions. One portion was combined with a portion of two other populations to form a pool of three populations. The pooled worms and the second portion of each population were used for DNA isolation. The third portion of each population was transferred to a fresh NGM plate and held for sib selection.

PCR-based screen to identify a *src-1* deletion. DNA isolated from the pools of mutagenized worms was screened for the presence of a deletion within *src-1* using PCR. Nested PCR primer pairs in exon three and exon six (JC98, JC99, JC61, JC62, see Table 3) and exon four and exon six (JC112, JC113, JC61, JC62) were used to amplify genomic *src-1* DNA. In both cases, the wild-type product is too large (approximately 6.5kb and 5kb respectively) to be amplified under the reaction conditions described. Only a large deletion within the confines of the primer pairs would provide a template of a size small enough for PCR amplification. When a PCR product was amplified from pooled DNA samples, the individual DNA samples comprising the pool were screened in duplicate. If the same PCR product was amplified from an individual DNA sample, it was considered to represent a candidate deletion. The held portion of the deletion positive population was then subjected to sib selection while the PCR product was sequenced to confirm the presence of a deletion.

Sib selection. Based on established protocols for sib selection (Rushforth et al., 1993; Zwaal et al., 1993), the held portion of deletion positive populations (which are expected to contain only a few of the desired mutants) were subdivided among 50-75 NGM

plates. After the next (F3) generation had emerged, each subpopulation was split into two halves. One half was used for DNA isolation followed by PCR and the second half was held on a fresh NGM plate. Subpopulations that were determined to be positive for the deletion were repeatedly subdivided and rescreened in the same manner in order to enrich for the desired mutant. After numerous rounds of subdivision, populations are enriched to the point that individual mutant worms are isolated.

RNA Isolation.

Six worms were picked to 5 μ l of RNase-free distilled water to which 50 μ l of GITC buffer (4M guanidinium thiocyanate, 50mM Tris-HCl pH 7.4, 50mM EDTA, 1% sarkosyl) was added. The samples were incubated in a dry ice / ethanol bath for 15 minutes. After thawing for one minute at 65°C, the samples were lyophilized. The dried pellet was resuspended in distilled water, phenol extracted, chloroform extracted, and finally precipitated with one tenth volume of 3.5M sodium acetate and three volumes of ethanol. All samples were resuspended in 20 μ l of distilled water and stored at -20°C.

Reverse Transcription - PCR.

An 11 μ l reverse transcription reaction contained the following:

2.5 μ l RNA
1 μ l (1mg) random or oligodT primers
9 μ l distilled water

Reactions were incubated at 70°C for five minutes then cooled on ice before addition of the following:

5 μ l 5X buffer
2.5 μ l 10mM dNTPs
1 μ l RNasin (40u)

2.5µl 40mM sodium pyrophosphate

1.5µl AMV-RT (13.5u)

Reactions were incubated at 37°C for 75 minutes. 1µl of the reverse transcription reaction was used for PCR with gene-specific primers as described above.

Directed Two-Hybrid Analysis.

Three independent GAL4-*src-1* fusions were constructed. The fusion protein encoded by each clone was tested for its ability to interact with a Gal4p-WRM-1 fusion protein (obtained from the Mello laboratory) in a directed two-hybrid assay.

Construction of GAL4-SRC-1 fusions. Primer JC194 was designed to incorporate an NcoI restriction site upstream of *src-1* and primer JC195 was designed to incorporate an XhoI restriction site downstream of *src-1*. The location of the NcoI restriction site was designed so that *src-1* would be cloned in frame with the activation domain of GAL4. The PCR product amplified from pCeSrc template DNA (*src-1* cDNA cloned into the EcoRI site of pBluescript-SK) was enzymatically digested according to manufacturer guidelines (Promega) and directionally cloned into the matching restriction sites within the pACT2 vector (Clontech) using T4 DNA polymerase according to manufacturer guidelines (Promega). The clones were transformed into DH5α cells according to manufacturer guidelines (Gibco-BRL) and selected by growth on LB-AMP plates (0.17M NaCl, 0.04mg/ml ampicillin; 10g tryptone, 5g yeast extract, 15g agar per 1L). Plasmids TW43, TW44, and TW49 were demonstrated to contain the *src-1* insert by enzymatic digestion with EcoRI which releases a 547bp fragment from within *src-1*.

Yeast DNA Transformation. Fresh yeast cells (20 - 50µl per transformation) of strain HF7c (Clontech) were washed with distilled water before resuspending in 100mM lithium acetate (LiAc) and incubating for five minutes at 30°C. At the end of the incubation period, the following components were added to the top of each cell pellet:

240µl PEG (50% w/v)
36µl 1M LiAc
25µl single stranded DNA (2.0mg/ml)
5µl plasmid DNA (approximately 5µg)
45µl distilled water

The transformation mixture was vortexed for at least one minute to resuspend the cell pellet before incubating at 42°C for 20 minutes. At the end of the incubation period, the cells were pelleted at top speed in a microcentrifuge then resuspended in 200µl of distilled water. The suspended cells were plated on the appropriate synthetic complete (SC) drop-out medium (2% glucose; 4g Difco Yeast Nitrogen Base without amino acids, 0.4g synthetic complete drop-out mix, and 10g agar per 600ml distilled water) to select for the presence of the plasmid. All plates were incubated at 30°C for three to four days until colonies were visible.

Histidine Reporter Assay. Yeast cells were streaked onto SC drop-out medium lacking leucine and tryptophan to select for presence of the plasmids. The medium also lacked histidine to test for activation of the HIS3 reporter. Included in the medium was 15mM 3-amino-1,2,4-triazole (3-AT), a competitive inhibitor of the His3p protein, to reduce background colony growth due to leakiness of the HIS3 reporter. All plates were incubated at 30°C for two days then assayed for colony growth.

β-galactosidase Assay. Yeast cells were streaked onto SC drop-out medium lacking leucine and tryptophan to select for presence of the plasmids. After incubating at 30°C for two days, colonies were lifted onto a nitrocellulose filter. The filter was submerged in liquid nitrogen until the cells were frozen then allowed to thaw at room temperature. This freeze / thaw treatment permeabilizes the cells. The thawed filter was incubated in 5ml of Z buffer / X-gal solution (0.1M NaHPO₄, 10mM KCl, 1mM MgSO₄•7H₂O, pH 7.0; 0.27% 2-mercaptoethanol, 0.33mg/ml X-gal) at room temperature then checked periodically for the appearance of blue colonies.

RESULTS

The goal of my dissertation research was to (1) establish that *src-1* is a *c-src* ortholog and (2) to determine the role of *src-1* in *C. elegans* development by isolating a loss-of-function allele of this gene. The information obtained from this study provides important insight into the normal biological role of this evolutionarily conserved tyrosine kinase. This in turn may shed light on its role in cancer.

Analysis of SRC-1 Phosphorylation.

The predicted SRC-1 protein contains all hallmarks of Src-family tyrosine kinases including Src homology 2 (SH2) and Src homology 3 (SH3) domains important for protein-protein interactions, a Src-family kinase domain, and a short C-terminal tail implicated in negative regulation of kinase activity (Figure 1). Several critical residues conserved among Src-family kinases are found in SRC-1, including: glycine 2, important for myristylation-mediated membrane localization; arginine 175 (R165 in SRC-1) which mediates interactions between the SH2 domain and tyrosine phosphorylated targets as well as its own tyrosine phosphorylated tail; lysine 295 (K290 in SRC-1), essential for ATP-binding and catalytic activity; and tyrosines 416 and 527 (Y528 in SRC-1), targets of phosphorylation important for regulation of catalytic activity. SRC-1 shares 45% overall sequence identity with chicken pp60^{C-src} (Takeya and Hanafusa, 1983) the most closely related vertebrate protein. Sequence conservation is highest (57% identity) across the kinase domains of these proteins (Figure 2).

Based on the conservation of key domains and amino acids between SRC-1 and c-Src, it seems likely that the two proteins share similar functions and modes of regulation. Vertebrate pp60^{C-src} activity is regulated by phosphorylation of tyrosine residues 416 and

Figure 1 - Predicted SRC-1 protein structure.

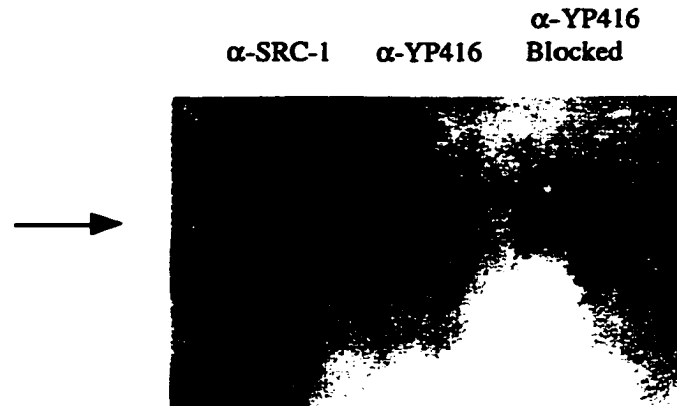


Legend: This figure is a cartoon representation of the *C. elegans* SRC-1 protein. The SH3, SH2, and kinase domains are boxed. The position of critical amino acids conserved among all Src-family members are indicated. These residues include: glycine 2, important for myristylation-mediated membrane localization; arginine 165 which mediates interactions between the SH2 domain and tyrosine phosphorylated targets as well as its own tyrosine phosphorylated tail; lysine 290, essential for ATP-binding and catalytic activity; and tyrosines 416 and 528, targets of phosphorylation important for regulation of catalytic activity. The function of each residue is assumed based on known properties of vertebrate pp60^c-src.

527. Phosphorylation of tyrosine 416 is specifically associated with activation of pp60^{C-src} (Kmieciak and Shalloway, 1987; Piwnica-Worms et al., 1987). To determine if SRC-1 is normally tyrosine phosphorylated, I immunoprecipitated the protein from wild-type *C. elegans* extracts using a SRC-1 specific antibody (Thacker and Capecchi, personal communication). Western blotting with an anti-phosphotyrosine antibody (monoclonal 4G10, Upstate Biotechnology) detects a protein of approximately 60 Kd, the size predicted for SRC-1 (Figure 3, lane 1). This result demonstrates that SRC-1 is normally phosphorylated on at least one tyrosine residue. To determine if the tyrosine 416 site is phosphorylated, I developed an antibody specific for this sequence. To generate this antibody, I synthesized a peptide antigen modeled on the tyrosine 416 region of SRC-1. The sequence of the peptide is as follows: Lys-Leu-Met-Glu-Glu-Asp-Ile-PTyr-Glu-Ala-Arg-Thr-Gly-Ala-Lys. This peptide was synthesized on an Applied Biosystems Model 431A peptide synthesizer. To confirm its composition, the peptide was analyzed by mass spectrum analysis performed by Mass Search Company (Figure 4) and sequenced using a Porton Instruments Model 2090 automated sequencer (Figure 5). After producing and purifying sera raised against this antigen, an indirect enzyme-linked immunosorbent assay (ELISA) was used to demonstrate the specificity of the antibodies. Purified sera reacted with the phosphorylated antigen but not with a corresponding non-phosphorylated peptide nor a phosphorylated peptide modeled on the tyrosine 416 region of pp60^{C-src} (Figure 6).

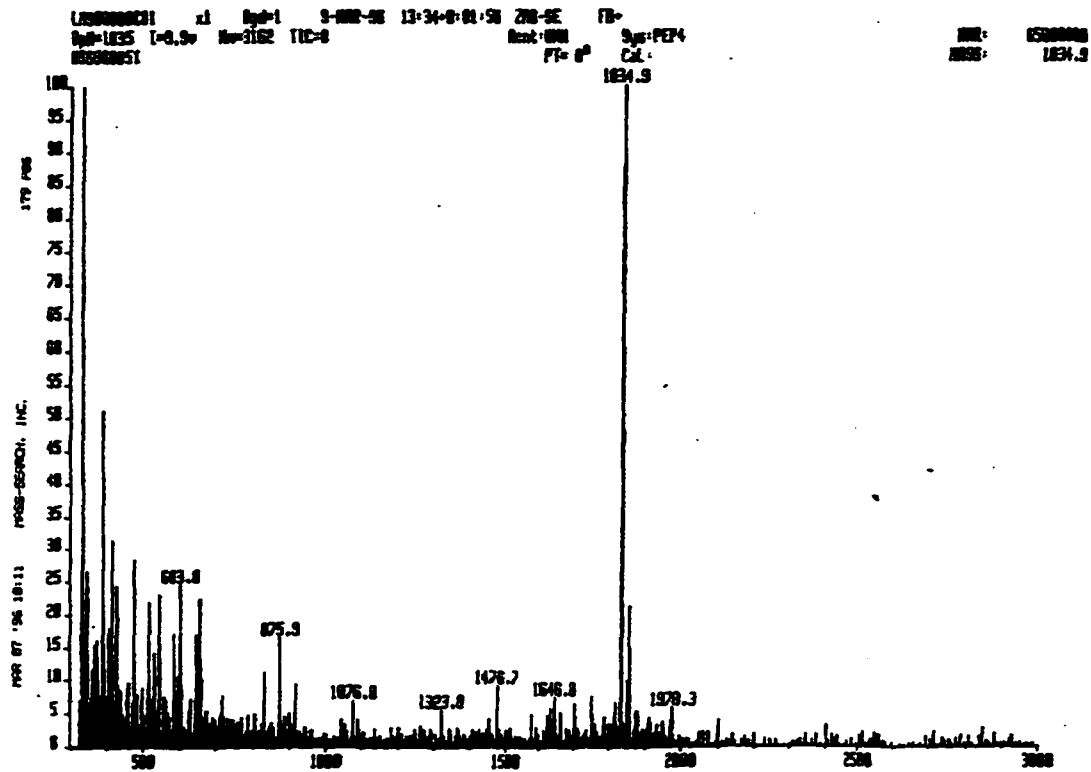
To determine if SRC-1 is phosphorylated on tyrosine 416, this antibody was used to immunoprecipitate wild-type SRC-1 from *C. elegans* extracts. Western blotting with the anti-phosphotyrosine antibody detected the same 60 Kd protein (Figure 3, lane 2) demonstrating that at least some fraction of SRC-1 is phosphorylated on tyrosine 416 *in vivo*. Specifically, this result demonstrates that some fraction of SRC-1 is normally maintained in a state of phosphorylation that is associated with catalytic activity of vertebrate pp60^{C-src}. Furthermore, this result suggests that the nematode and vertebrate proteins are subject to similar forms of post-translational regulation and provides additional evidence in support of the hypothesis that SRC-1 and pp60^{C-src} are orthologs that function

Figure 3 - Analysis of the phosphorylation state of wild-type SRC-1.

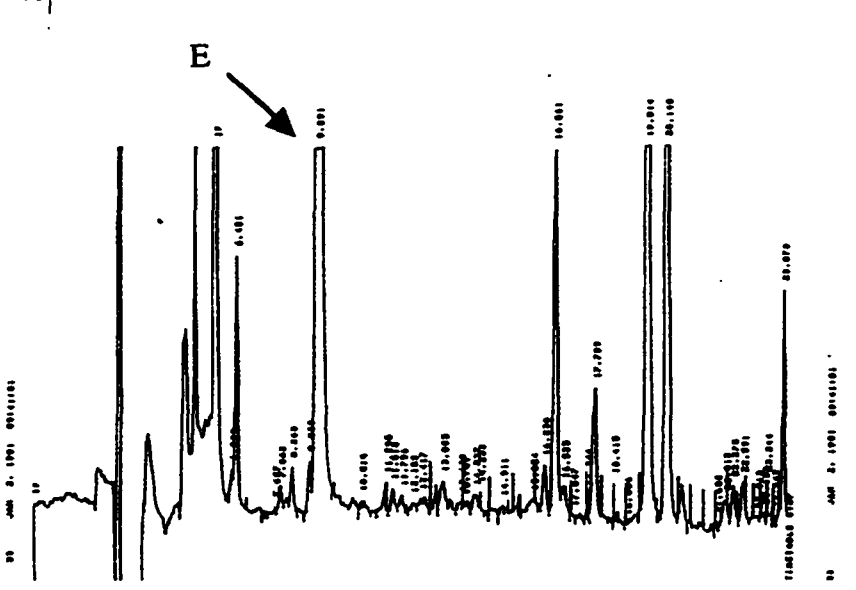
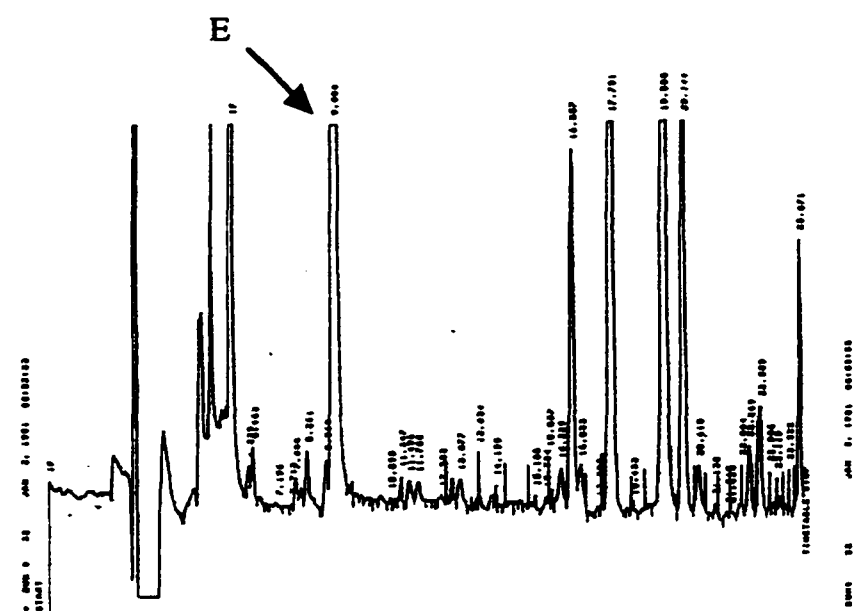
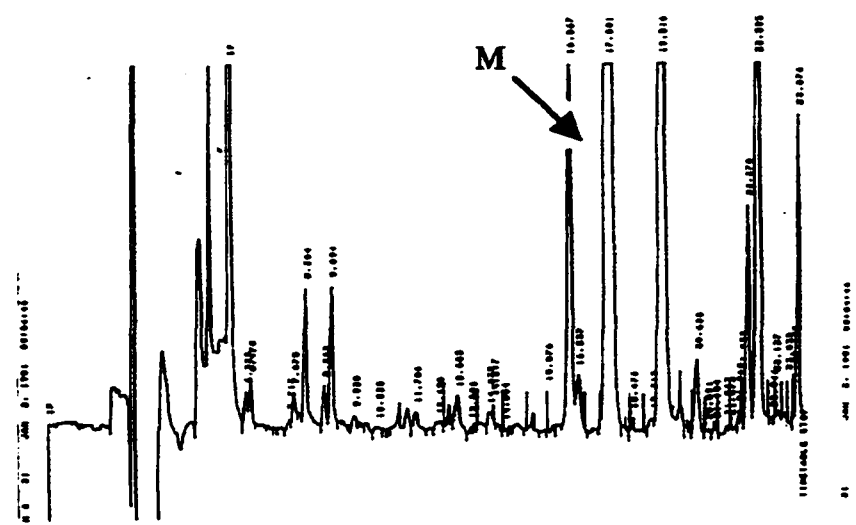


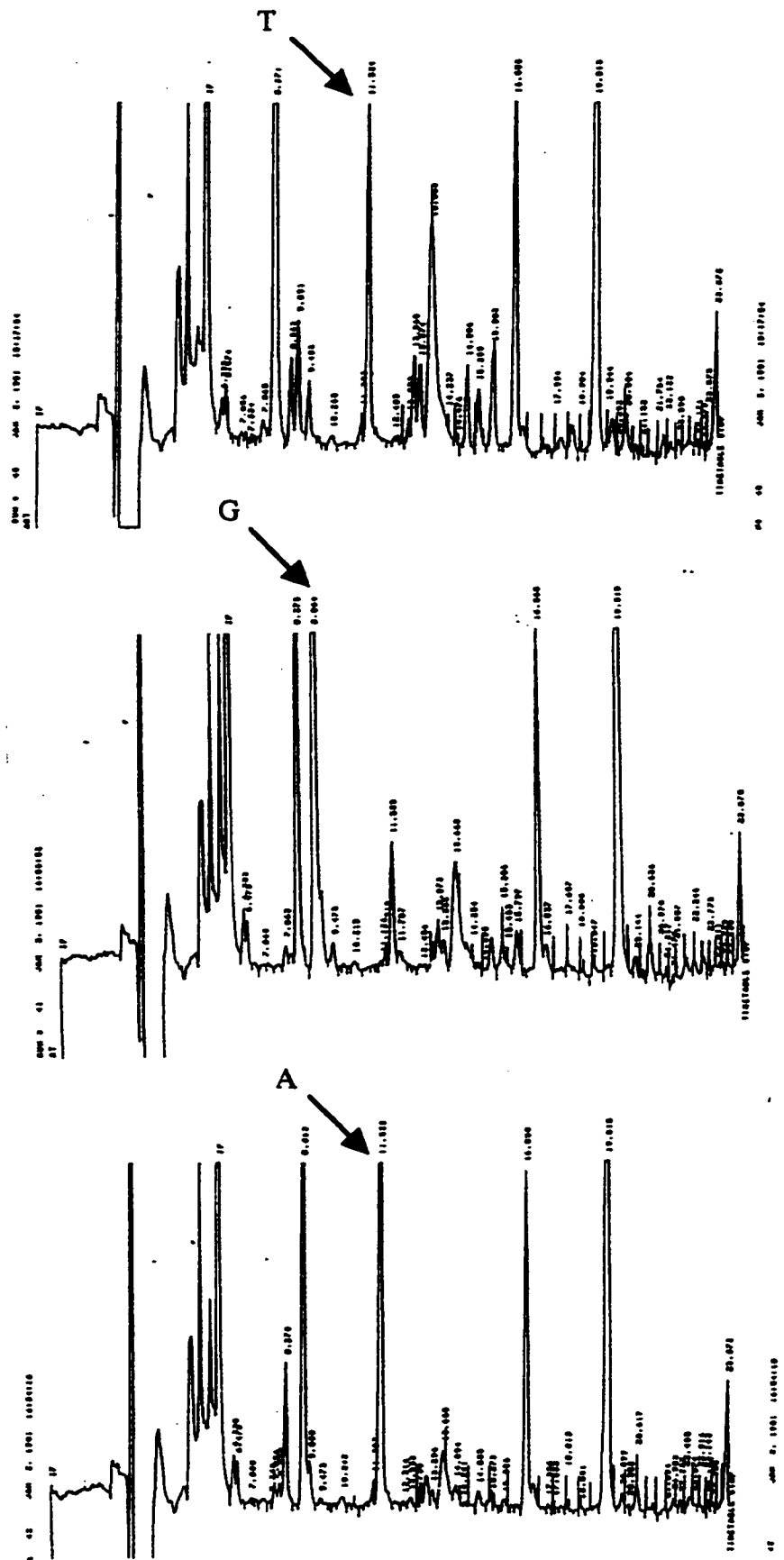
Legend: This figure depicts a western blot of wild-type N2 extracts using a commercial anti-phosphotyrosine antibody (Upstate Biotechnology). The sample in lane 1 was immunoprecipitated with anti-SRC-1 (Thacker and Capecchi, personal communication). Samples in lanes 2 and 3 were immunoprecipitated with anti-PY416SRC-1. Both SRC-1 antibodies immunoprecipitate a protein of approximately 60 Kd (denoted by arrow). Immunoprecipitation is blocked by preincubation of anti-PY416SRC-1 with the peptide antigen as shown in lane 3.

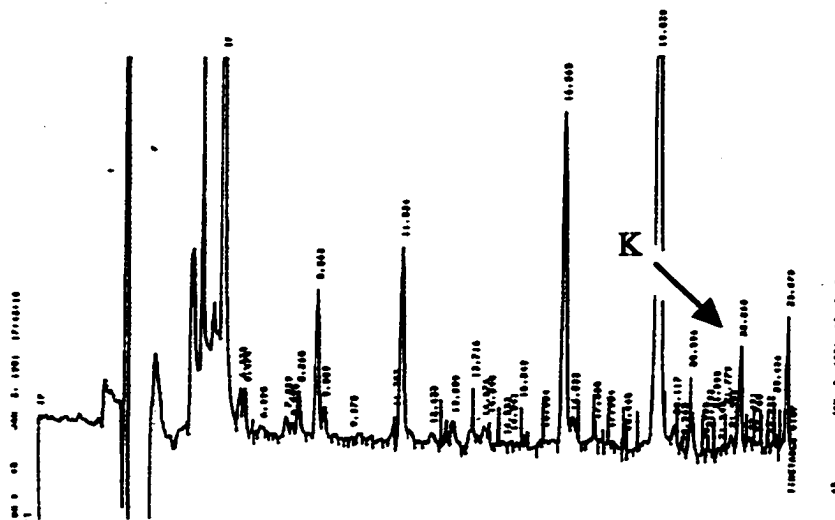
Figure 4 - Mass spectrum analysis of phosphorylated SRC-1 peptide.



Legend: Peak height indicates percent relative abundance. In this case, the peak of molecular weight 1834.9 represents the most abundant species. This is close to the predicted molecular weight of 1832.9.

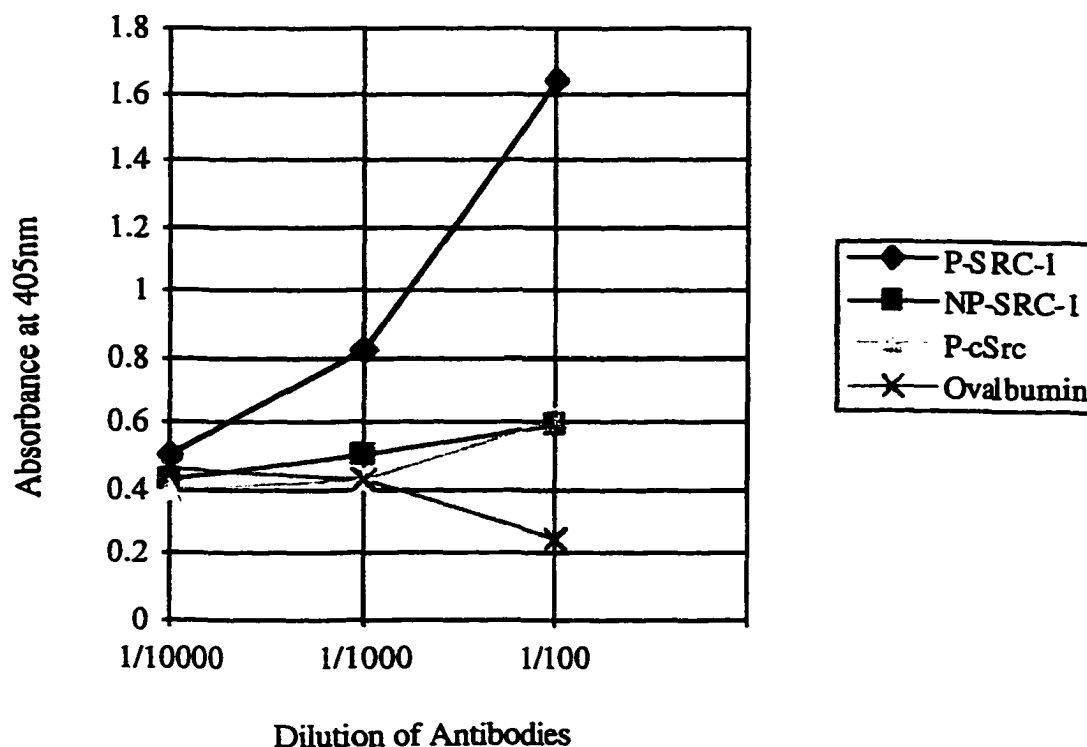






Legend: Each chromatograph represents one cycle of Edman degradation from N-terminus to C-terminus of the 15mer peptide. Arrows indicate the peaks which identify the amino acids detected for each cycle. These peaks were identified by comparison to a chromatograph of amino acid standards. No peak is evident for phosphotyrosine at cycle #8 because it is not resolved under the gradient condition employed. The peak identifying lysine in cycle #15 is very weak because it is the last amino acid remaining and most had likely washed off the chromatographic membrane to which the peptide was originally applied. This analysis confirms that the sequence of the peptide is Lys-Leu-Met-Glu-Glu-Asp-Ile-(P-Tyr)-Glu-Ala-Arg-Thr-Gly-Ala-Lys.

Figure 6 - Specificity of SRC-1 antibodies.



Legend: Specificity of the affinity purified sera was determined by indirect ELISA. This graph depicts the results obtained for fraction #1. The sera specifically bound to the phosphorylated peptide modeled on the tyrosine 416 region of SRC-1. Very little binding above background (represented by ovalbumin) was observed with either the non-phosphorylated peptide modeled on the tyrosine 416 region of SRC-1 or the phosphorylated peptide modeled on the tyrosine 416 region of pp60^{c-src}.

similarly in these distantly related organisms.

Mapping *src-1*.

The primary goal of my dissertation research was to determine the role(s) of *src-1* in *C. elegans* development. To achieve this goal, I sought to identify a *src-1* loss-of-function mutant. The phenotype of this mutant would reveal the normal function of SRC-1 and provide a starting point for elucidating the signaling pathways through which SRC-1 acts. I employed two approaches to identify a *src-1* mutant: (1) using a candidate gene approach, I mapped *src-1* and examined the identified genomic region for known genes with phenotypes suggesting they might actually be *src-1*; and (2) I used a PCR-based assay to screen for a *src-1* deletion mutant induced by chemical mutagenesis. This section describes the mapping of *src-1*.

Mutants that I would consider as potential *src-1* alleles would be those with phenotypes similar to those seen in vulval induction and sex myoblast migration pathway mutants. Both of these pathways utilize the conserved MAP-kinase pathway of which *src-1* would be predicted to be a member (Sundaram and Han, 1996; Sundaram et al., 1996). Because decreased signaling through these pathways leads to a vulvaless (Vul) or egg-laying defective (Egl) phenotype, I considered these types of mutants promising candidates for a *src-1* allele.

At the time this work was undertaken, a detailed physical map of the *C. elegans* genome was essentially complete. The entire genome was represented in an overlapping set of yeast artificial chromosome (YAC) clones that were available as a grid. Probing this grid with fragments of the *src-1* gene had previously failed to identify, unambiguously, a YAC containing *src-1* sequence (Thacker and Capecchi, personal communication). While the *src-1* probes did hybridize to a large contig that presumably contained *src-1* sequences, the *C. elegans* genome sequencing consortium had never been able to place this “orphaned” contig on the physical map. Clearly, *src-1* sequence must be contained within a gap on the

physical map, but such gaps were scattered across all six chromosomes. To identify where *src-1* resides within the genome, I mapped the gene using standard linkage analysis in combination with a PCR assay.

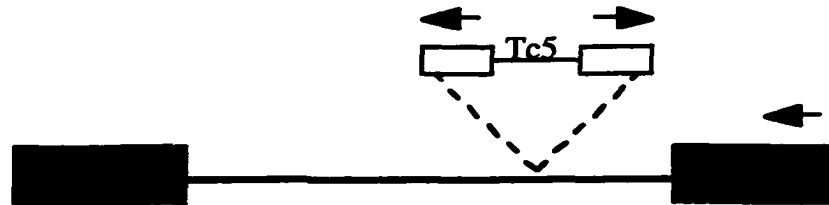
For the mapping experiments I used *src-1(cj290::Tc5)*, an allele containing an insertion of the transposable element Tc5 within the fifth intron of the gene (Zhang, 1996). While there is no phenotype associated with this transposon insertion, it provides a molecular marker for tracking segregation of *src-1*. PCR using a Tc5-specific primer (JC70) in combination with a *src-1*-specific primer (JC62) amplifies a 1.2 Kb product from *src-1(cj290::Tc5)* template DNA (Figure 7). No product is amplified from wild-type *src-1* template DNA. Because this molecular assay provided the means to distinguish between the mutant and wild-type alleles of the gene, I was able to use standard two point linkage analysis to map *src-1*.

Linkage group X was tested by taking advantage of the XO genotype of males. In the wild, *C. elegans* are mainly found as self-fertile hermaphrodites which carry two X chromosomes. Males naturally arise at a low frequency due to non-disjunction during meiosis. Thus, males carry only one X chromosome. When a male (XO) is mated to a hermaphrodite (XX) 50% of cross progeny will receive an X chromosome from the male parent (these are XX hermaphrodites) and 50% of cross progeny will not receive an X chromosome from the male parent (these are XO males). Thus, males carrying an X-linked mutation are unable to transmit the mutation to male progeny. Heterozygous *src-1(cj290::Tc5)* males mated to wild-type hermaphrodites transmitted the marked allele to 33% of their male progeny. This result clearly demonstrates that *src-1* does not reside on linkage group X.

To test the five autosomes for linkage, a genetic marker was chosen for the right, middle, and left region of each and introduced into the *src-1(cj290::Tc5)* background using standard genetic crosses. The crosses were designed so that if the chosen marker and *src-1* are unlinked, 75% of progeny homozygous for the marker are expected to also segregate *src-1(cj290::Tc5)* (50% will be heterozygous for the insertion allele and 25% will be

Figure 7 - Strategy for following segregation of *src-1(cj290::Tc5)*.

(A)



(B)



Legend: Both cartoons depict the region of *src-1* sequence that spans from exon five to exon six. Exon sequence is represented by black boxes and intron sequence is represented by a line. The inverted repeats of the transposon are represented by empty boxes. The site of insertion is indicated by the dashed lines. Arrows indicate the location of primers. Panel (A) depicts *src-1(cj290::Tc5)*. Note that the Tc5-specific primer (JC70) and *src-1*-specific primer (JC62) will amplify a PCR product. Panel (B) depicts wild-type *src-1*. Without the transposon insertion in intron five, the *src-1*-specific primer (JC62) fails to amplify a PCR product. Thus this PCR assay can distinguish which alleles are present in preparations of genomic DNA.

homozygous). If the chosen marker and *src-1* are tightly linked, none of the homozygous progeny are expected to also segregate *src-1(cj290::Tc5)*. However, recombination will likely result in an actual segregation rate of greater than zero percent for linked mutations. PCR analysis of cross progeny showed that for each marker except one, approximately 75% of homozygous progeny co-segregated the Tc5-tagged allele of *src-1* (Figures 8 and 9a). In contrast, only 5% of *bli-3(e767)* homozygotes co-segregated *src-1(cj290::Tc5)* (Figures 8 and 9b) suggesting that *src-1* is located in close proximity to *bli-3* on the left arm of linkage group I. Subsequent PCR analysis with a pair of unrelated primers in *unc-22* confirmed that the negative reactions observed for 95% of the *bli-3(e767)* homozygotes was due to absence of the Tc5-tagged *src-1* allele and was not due to missing or degraded template DNA. Looking more closely at the rate of co-segregation obtained for *dpy-5(e61)* homozygotes (47%), the marker at the middle of linkage group I, further supports the conclusion that *src-1* resides on the left arm of linkage group I. 47% is significantly different from 75% (chi square analysis) suggesting that *src-1* and *dpy-5* are indeed linked. If *src-1* resides near *bli-3* (the recombination frequencies would suggest a distance of +/- five map units), as much as 20 map units could separate *src-1* and *dpy-5*. This large physical distance between the two genes would lead to frequent recombination events that could result in the high rate of co-segregation observed. Collectively, the data support the conclusion that *src-1* maps to the left arm of linkage group I. Armed with this genetic evidence placing *src-1* on the left arm of linkage group I, the *C. elegans* genome sequencing consortium reexamined the location of *src-1* on the physical map. Their analysis confirmed my mapping data and located *src-1* on YAC Y92H12 approximately four map units to the right of *bli-3* (Coulson, personal communication).

Unfortunately, the map position did not help my efforts to identify a *src-1* mutant. The left arm of linkage group I is a very gene poor region of the genome that doesn't offer any likely candidates for a *src-1* mutant. Among the genes mapped to this region are *spe-8*, *spe-13*, and *spe-15*, all of which are defective in some aspect of spermatogenesis (L'Hernault et al., 1988); *smg-2*, a gene involved in nonsense mediated decay of mRNA

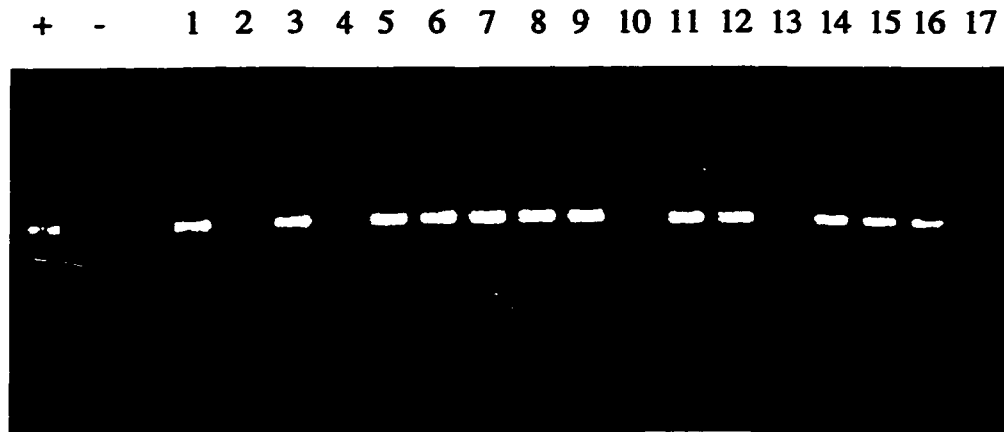
Figure 8 - *src-1(cj290::Tc5)* co-segregation frequencies.

	L	M	R
I	<i>bli-3(e767)</i> 5%	<i>dpy-5(e61)</i> 47%	<i>unc-54(r323)</i> 68%
II	<i>sqt-2(sc108)</i> 60%	<i>dpy-10(e128)</i> 74%	<i>unc-52(e444)</i> 78%
III	<i>dpy-1(e1)</i> 68%	<i>unc-36(e251)</i> 63%	<i>bli-5(e518)</i> 64%
IV	<i>dpy-9(e12)</i> 80%	<i>unc-22(r644)</i> 57%	<i>dpy-4(e1166)</i> 73%
V	<i>unc-34(e315)</i> 67%	<i>dpy-11(e224)</i> 72%	<i>unc-51(e369)</i> 87%

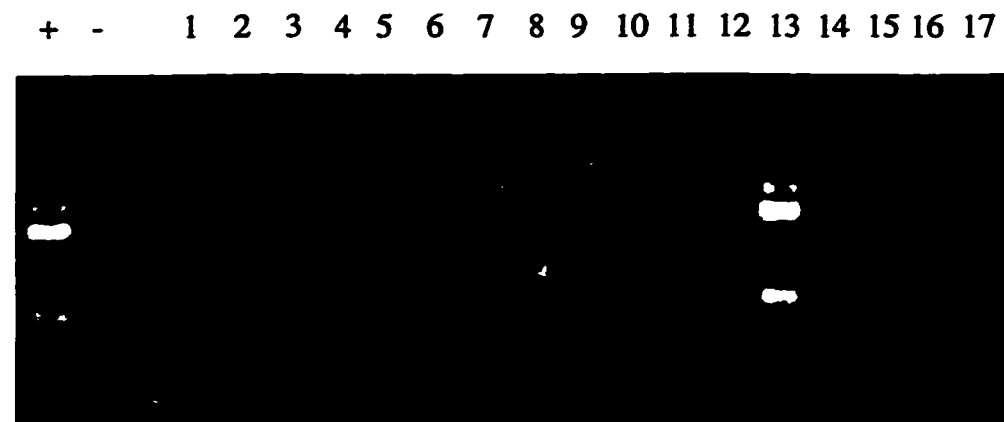
Legend: Genetic markers chosen for testing linkage of *src-1* to the left, middle, and right arms of autosomes I through V are shown with the allele number in parentheses. The percentage of F2 progeny homozygous for each marker that also segregated the *src-1(cj290::Tc5)* allele is indicated below each individual marker tested. Only *bli-3(e767)* individuals demonstrated a percent co-segregation close to zero as expected for linked traits.

Figure 9 - PCR scoring of *src-1(cj290::Tc5)* co-segregation.

(A)



(B)



Legend: Panel (A) depicts the results of PCR performed on 17 *dpy-10(e128)* homozygous F2 individuals. 12/17 individuals (71%) also segregated *src-1(cj290::Tc5)*. In contrast, panel (B) depicts the results of PCR performed on 17 *bli-3(e767)* homozygous F2 individuals. Only 1/17 individuals (6%) also segregated *src-1(cj290::Tc5)* indicating that *bli-3* and *src-1* are closely linked.

(Hodgkin et al., 1989); and *spn-1*, which exhibits a reversal of handedness in developing embryos (Wood, 1998). None of the phenotypes exhibited by these mutants resembled the Egl or Vul phenotypes predicted for *src-1*. The only gene in the region which fit the predicted phenotype, *egl-30*, had previously been cloned and shown to encode a heterotrimeric G protein (Brundage et al., 1996). In the absence of any promising candidates, I shifted my focus to isolating a *src-1* mutant using a reverse genetic approach.

Isolation of a *src-1* Deletion Mutant.

Despite the transposon insertion within the fifth intron of the gene, *src-1(cj290::Tc5)* encodes a wild-type mRNA as Tc5 sequence is removed via splicing (Zhang, 1996). As a result, this mutant does not exhibit a phenotype. However, this mutant does provide a starting place for a transposon-based approach to isolating a *src-1* loss-of-function allele. Tc5 transposons are known to excise from genomic sequences in a *mut-2(r459)* background (Collins and Anderson, 1994). Nearly all excision events are imprecise leaving a small, characteristic “foot print” that usually does not disrupt gene function. However, some excision events result in deletion of large regions of sequence surrounding the insertion site. An excision event that resulted in deletion of exon sequence downstream of the Tc5 insertion site in *src-1* would likely disrupt gene function. Towards this end, strain TW411 was constructed by crossing *mut-2(r459)* into the *src-1(cj290::Tc5)* background. In excess of 1.2×10^6 haploid *src-1(cj290::Tc5)* genomes were screened for Tc5 excision events using a previously described PCR-based assay (Zhang, 1996). A number of deletion alleles were identified by PCR and confirmed by DNA sequence analysis. However, none of these alleles were ever recovered in individual animals. Eventually, I abandoned this transposon-based approach to mutagenesis in favor of a new approach which relied on a chemical mutagen to directly induce a deletion in the targeted gene.

A number of mutagens have been tested for their ability to induce deletions. Based

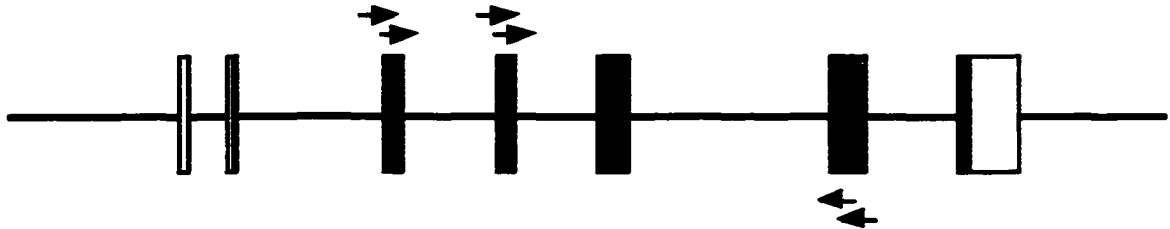
on the frequency of mutagenesis and the availability of a straight forward protocol, I chose to use *N*-ethyl-*N*-nitrosourea (ENU). Using the *unc-93* locus as a model, this mutagen has a demonstrated mutagenesis rate of 3×10^{-4} per haploid genome (DeStasio et al., 1997). Because intragenic deletions represent only 13% of all ENU-induced mutations at the *unc-93* locus (DeStasio et al., 1997), the frequency at which deletions occur is predicted to be 4×10^{-5} per haploid genome. Despite a 10-fold lower rate of occurrence, this class of mutation is desirable for two reasons: (1) it is likely to result in a loss-of-function allele and; (2) it can be readily identified in a background of wild-type alleles using PCR.

In order to be able to identify an ENU-induced deletion at the *src-1* locus, I designed two sets of nested primers to span a genomic region of 5 Kb and 6.5 Kb respectively (Figure 10). Only a large deletion within the boundaries of either set of primers would generate a DNA template small enough (< 3 Kb) to be amplified under the PCR conditions used. Within screening 3×10^4 haploid, ENU mutagenized genomes (see Materials and Methods), the mutant allele designated *src-1(cj293)* was identified in a single population as an approximately 2 Kb PCR product (Figure 11). Because this product was amplified with the set of primers spanning 6.5 Kb of wild-type *src-1* sequence, it appeared to represent a 4.5 Kb deletion. After six rounds of sib selection (see Materials and Methods) (Rushforth et al., 1993; Zwaal et al., 1993), individual worms heterozygous for *src-1(cj293)* were isolated.

Molecular Characterization of *src-1(cj293)*.

PCR and DNA sequence analysis determined that the *cj293* lesion is an approximately 4.5 Kb deletion that extends from the third to the fifth intron of *src-1* (Figure 12). Because *src-1* intron sequence is not known, I have not defined the end points of the lesion. However, exons four and five, which encode the SH2 domain and N-terminal portion of the kinase domain, including the conserved ATP-binding site (K290), are completely removed. Deletion of these sequences ensures that *src-1(cj293)* is a kinase

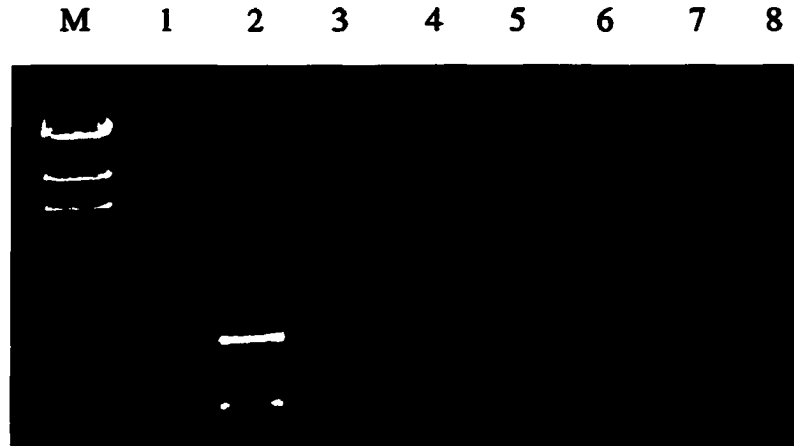
Figure 10 - *src-1* deletion screen strategy.



Legend: This cartoon depicts the exon/intron structure of wild-type *src-1*. The line represents intron sequence and the boxes represent exon sequence. Empty boxes represent non-coding sequence and shaded boxes represent coding sequence. The location of primers are denoted by arrows. Nested primer pairs in exons four (JC112, JC113) and six (JC61, JC62) and exons three (JC98, JC99) and six (JC61, JC62) were designed to amplify genomic fragments of 5 kb and 6.5 kb respectively. Both fragments are too large to amplify under the PCR conditions used. Only a deletion within the boundaries of a primer set will produce a template small enough to be amplified under the PCR conditions used.

Figure 11 - Identification of *src-1(cj293)* as a PCR product.

(A)

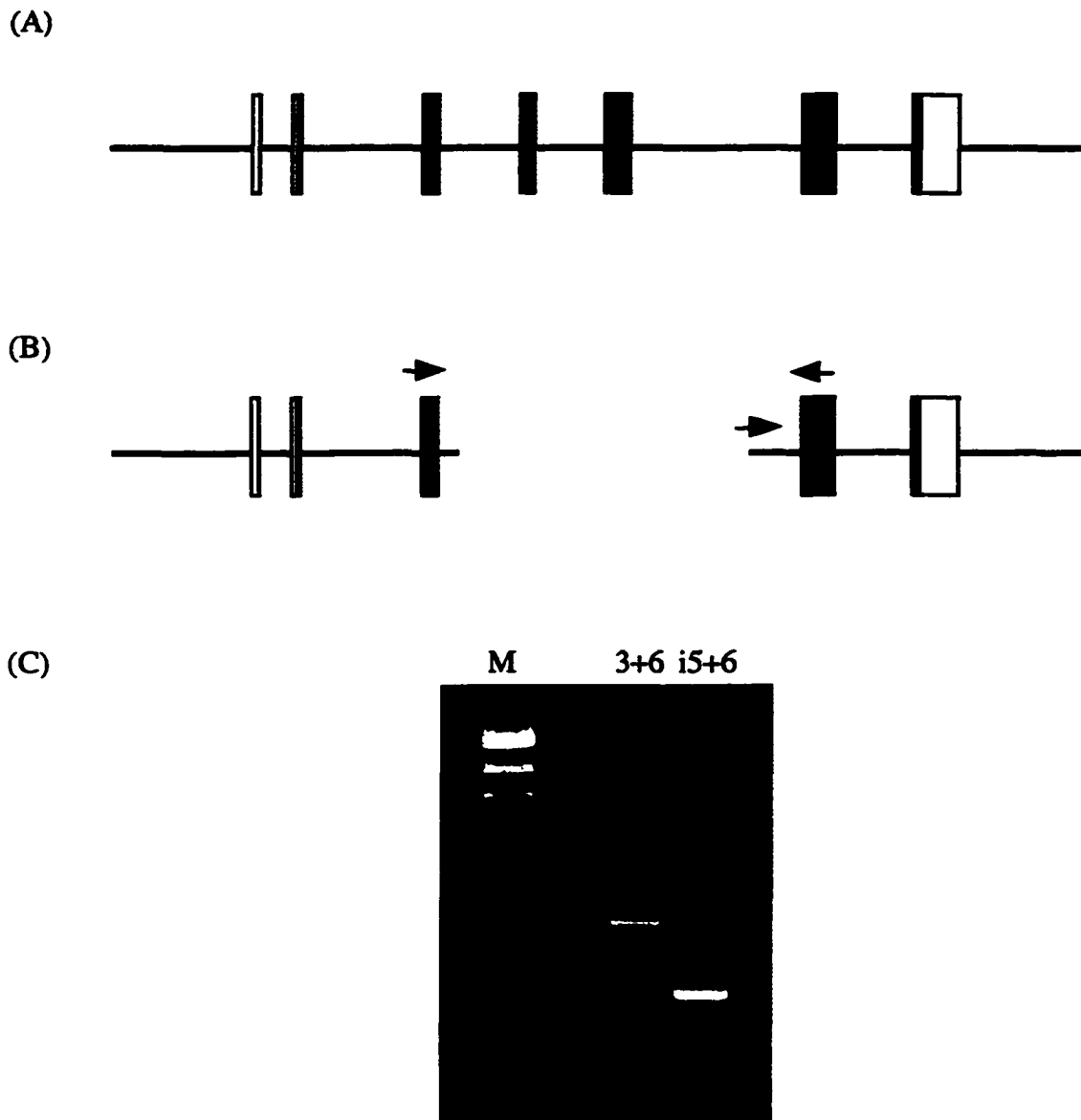


(B)



Legend: Panel (A) shows the results of PCR analysis of eight pooled populations of ENU mutagenized worms using the nested primer pairs JC98 and JC62 followed by JC99 and JC61. Pool two amplifies a PCR product, the largest band being just less than 2 kb, suggesting that one of the populations represented in this pool contains individual worms harboring a *src-1* deletion. Panel (B) shows the results of PCR analysis of the three populations represented by pool two. The analysis was conducted in duplicate. As shown, pool two and population 2a amplify the same PCR product. Additional PCR analysis determined that the largest band is the true PCR product.

Figure 12 - Genomic structure of the deletion allele *src-1(cj293)* .



Legend: Figure (A) depicts the exon/intron structure of wild-type *src-1*. The line represents intron sequence and the boxes represent exon sequence. Empty boxes represent non-coding sequence and shaded boxes represent coding sequence. Figure (B) depicts the exon/intron structure of the deletion allele, *src-1(cj293)*, isolated by ENU mutagenesis. . As shown, the lesion endpoints extend from the third to the fifth intron completely removing exons four and five. Placement of the deletion endpoints is based on partial sequencing and the PCR analysis (primer locations are denoted as arrows) depicted in panel (C). Only primers located in exons three and six and the 3' end of intron five are able to amplify a PCR product from genomic *src-1(cj293)* DNA.

inactive allele. To determine if the allele is expressed, I performed RT-PCR on RNA from pools of *src-1(cj293)* homozygotes. My analysis revealed the presence of a *src-1* transcript, but this transcript appears to be cleaved and polyadenylated within the intron 3 / intron 5 fusion (Figure 13). This unspliced, fused intron introduces an opal (UGA) stop codon immediately downstream of the SH3 domain. The resulting 137 amino acid protein, if translated, would lack an SH2 domain, kinase domain, and C-terminal tail (Figure 14). Due to the certainty that this truncated protein would be catalytically inactive, I have concluded that *cj293* is a *src-1* knock-out allele.

Phenotypic Characterization of *src-1(cj293)*.

src-1(cj293) confers a recessive maternal effect lethal (Mel) phenotype; homozygous animals are viable because they receive a maternal supply of RNA or protein from the heterozygous parent, but their progeny are not. *src-1(cj293)* progeny arrest as embryos. This embryonic lethality is completely penetrant: 100% of embryos born from homozygous *src-1(cj293)* mothers fail to hatch (Table 4). The maternal effect is not strict, however, since I observed low levels of zygotic rescue when *src-1(cj293)* homozygotes were cross fertilized by N2 males (Table 4). Interestingly, heterozygous cross progeny that escape arrest show a spectrum of phenotypes including larval lethality, arrested development, and sterility (Table 5). Rare wild-type, fertile adults are also observed. While the range of phenotypes seen in zygotically rescued heterozygotes suggest that SRC-1 may have additional roles beyond its essential role in embryogenesis, these phenotypes are never seen in *src-1(cj293)* homozygotes born from heterozygous mothers.

Figure 13 - RT-PCR analysis of a *src-1(cj293)* transcript.

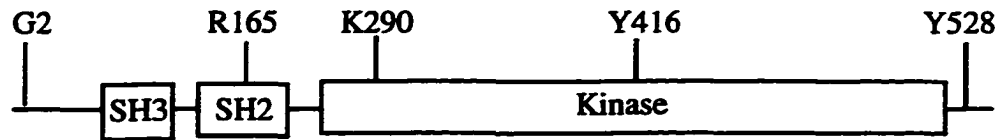
Exons 3 & 6		Exon 3		Exon 6	
N2	<i>cj293</i>	N2	<i>cj293</i>	N2	<i>cj293</i>



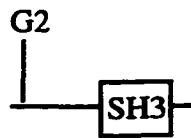
Legend: RT-PCR was used to test for the presence of a *src-1(cj293)* transcript. Following a reverse transcription reaction using random hexamer primers, PCR was performed using nested primers spanning the *cj293* lesion (JC98 and JC62; followed by JC99 and JC61). While a transcript was detected from the wild-type sample, this analysis failed to identify a transcript from the *src-1(cj293)* sample. One explanation for such a result is that no transcript is made from the mutant allele. A second explanation is that the transcript is made, but the fused intron is not spliced leading to a truncated message that does not contain exon sequence downstream of the lesion. To distinguish between these possibilities, PCR was repeated using a pair of semi-nested primers contained in exon three (JC98 and JC155; followed by JC99 and JC155) in one reaction and a pair of semi-nested primers contained in exon six (JC156 and JC62; followed by JC156 and JC61) in another reaction. As shown in the figure, this PCR analysis demonstrates the presence of a transcript that contains sequences from exon three but not from exon six suggesting that the transcript is indeed truncated.

Figure 14 - Proposed effect on *src-1(cj293)* protein if translated.

(A)



(B)



Legend: Figure (A) is a cartoon representation of the wild-type SRC-1 protein. Figure (B) is a cartoon representation of the predicted protein that may be encoded by *src-1(cj293)*. Greater than 75% of the protein would be missing. The deleted and untranslated sequences include both the SH2 and kinase domains ensuring that the protein would be catalytically inactive.

Table 4 - *src-1(cj293)* maternal effect lethality.

Mothers genotype	Embryos genotype	% Arrested (n)
<i>src-1(cj293)</i>	<i>src-1(cj293)</i>	100 (1382)
<i>src-1(cj293)</i>	<i>src-1(cj293)/+</i>	89.9 (2160)

Table 5 - Phenotypes of zygotically rescued *src-1(cj293)* heterozygotes.

Phenotype	% Observed (n)
larval lethal	19 (41)
arrested development	14 (31)
sterile adult hermaphrodite	28 (61)
wild-type adult hermaphrodite	9 (19)
adult male (fertility undetermined)	27 (60)

Note: Percentages do not add up to 100% because 3% (7) were unable to be scored.

The embryonic lethality of *src-1(cj293)* mutants makes propagation of the allele difficult. In order to maintain the allele in a heterozygous state, I balanced it versus the translocation *szT1(I;X)*. Because the translocated chromosome bearing the left arm of linkage group I pairs with linkage group X during meiosis, *src-1(cj293)* can not be lost by recombination (Fodor and Deak, 1982; McKim et al., 1988). The balanced strain, designated TW416, is successfully maintained as a heterozygote because all other progeny (*src-1(cj293)* homozygous progeny and aneuploid progeny lacking an intact linkage group

I or X) arrest as embryos. Using a different class of balancer, I constructed a second strain which allows *src-1(cj293)* to be maintained in a homozygous state. *sDp2(I;f)* is a free duplication of the left arm of linkage group I that is stably maintained extrachromosomally (Rose et al., 1984). The wild-type copy of *src-1* contained on *sDp2(I;f)* rescues the Mel phenotype of *src-1(cj293)* homozygotes. Because the duplication does not pair with linkage group I during meiosis, the mutant allele can not be lost by recombination. The balanced strain, designated as TW424, produces animals that have lost *sDp2(I;f)* at a low frequency (less than 5%). These *src-1(cj293)* homozygous animals that lose *sDp2(I;f)* are no longer rescued and their progeny arrest as embryos.

Because a chemical mutagen was used to isolate *src-1(cj293)*, it is important to show that the Mel phenotype does not result from a second, unrelated mutation in the background. To eliminate this concern, I backcrossed *src-1(cj293)* homozygotes by N2 wild-type males three times. F1 heterozygotes always reseggregated Mel progeny as expected. However, the Mel phenotype occasionally segregated away from a zygotic phenotype that was originally associated with the *src-1(cj293)* lesion. PCR analysis of individuals that no longer co-segregated the Mel phenotype determined that they were wild type at the *src-1* locus. This data demonstrates that a second mutation genetically linked to *src-1(cj293)* was isolated in the mutagenesis screen. This allele, designated *cj294*, produces a recessive squat, kinky, Egl-like phenotype that I refer to as Ske. It appears to be an allele of a new gene that may be of interest to someone studying muscle mutants. Due to the complexities of working with a Mel allele, I have not recovered *src-1(cj293)* outside of the *cj294* background.

The presence of this second mutation reinforced the concern that the Mel phenotype could be due to a closely linked, yet unrelated mutation separate from *src-1(cj293)*. To confirm that this is not the case, in collaboration with Yanxia Bei, a graduate student in Craig Mello's laboratory at the University of Massachusetts Medical Center at Worcester, Massachusetts, *src-1* was knocked-out by an independent method termed RNA-mediated interference (RNAi). RNAi has been shown to phenocopy loss-of-function mutations for a

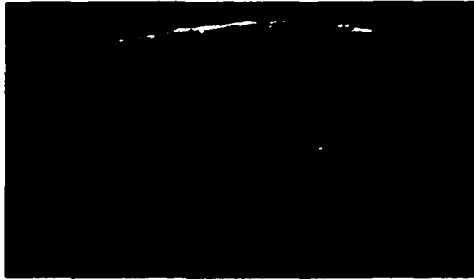
wide range of *C. elegans* genes tested (Guo and Kemphues, 1995, 1996; Lin et al., 1995; Mello et al., 1996; Powell-Coffman et al., 1996; Guedes and Priess, 1997; Rocheleau et al., 1997; Thorpe et al., 1997). While the mechanism behind the effect is unclear, protein expression from the target gene is eliminated in the progeny of injected worms (Lin et al., 1995; Powell-Coffman et al., 1996). Injection of *in vitro* synthesized *src-1* RNA into the gonad region of wild-type hermaphrodites produces progeny that exhibit an embryonic arrest phenotype indistinguishable from that of *src-1(cj293)* progeny. This result confirms that the Mel phenotype observed in *src-1(cj293)* mutants is caused by the *cj293* lesion and that maternal effect lethality represents a loss-of-function phenotype for *src-1*.

To obtain insight into the role SRC-1 is playing in embryonic development, I characterized the embryonic arrest phenotype in more detail in collaboration with Yanxia Bei from Craig Mello's laboratory. We characterized the cellular phenotype of the arrested embryos using light and immunofluorescence microscopy. Our analysis revealed that *src-1(cj293)* embryos exhibit a complete absence of morphogenesis. This defect appears to be due to failure of hypodermal cells to enclose the developing embryos. As a result embryos fail to elongate and instead develop as a sphere of cells (Figure 15). Differentiation does occur such that individual cell types including intestine, neuron, pharynx, and germline differentiate appropriately to produce cell type-specific markers. However, these tissues fail to become properly organized (Figure 15). At the time point beyond which hatching would normally occur, cell death becomes apparent. The absence of morphogenesis suggests that SRC-1 may play a role in cytoskeletal organization during embryogenesis. This theory is further supported by the observation that orientation of the mitotic spindle is disrupted in at least one cell type of *src-1(cj293)* embryos.

A second feature of *src-1(cj293)* embryos is that they appear to produce extra intestinal cells. The early cell divisions in *C. elegans* embryogenesis generate six blastomeres or "founder cells" each of which executes a unique pattern of cell divisions and cell fates (Figure 16). One of these cells, the E blastomere, gives rise to the organism's entire intestine and only the intestine. This cell type is easily identified by virtue of gut granule autofluorescence under plane-polarized light. Examination of arrested embryos

Figure 15 - *src-1(cj293)* embryos exhibit defective morphogenesis.

(A) Wild type



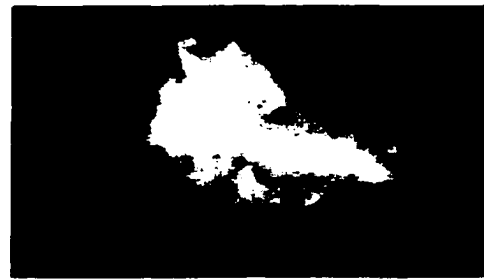
(B) *src-1(cj293)*



(C) Wild type

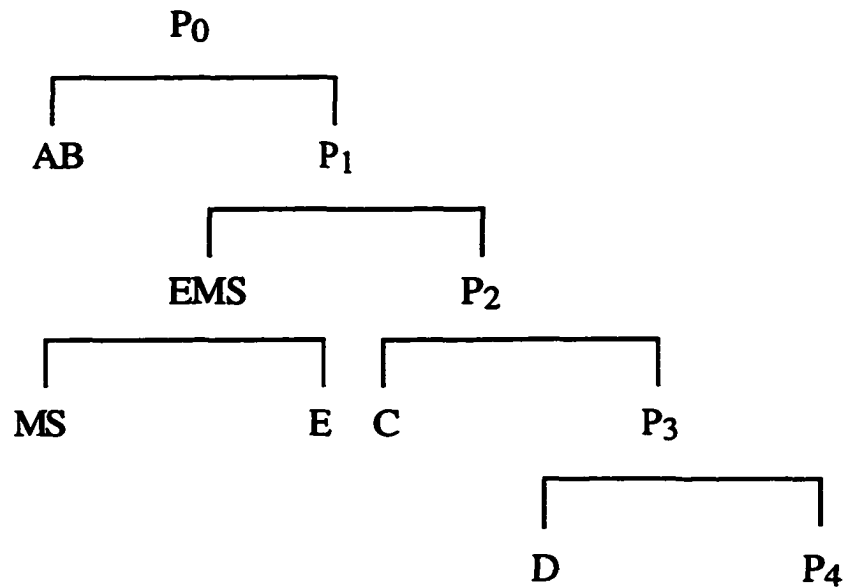


(D) *src-1(cj293)*



Legend: The pictures shown in this figure were taken by Yanxia Bei. Panels (A) and (B) are light micrographs of living embryos. The wild-type embryo (A) has initiated morphogenesis and will ultimately elongate four-fold before hatching. The *src-1(cj293)* embryo (B) has not initiated morphogenesis despite being past the time point at which hatching normally occurs. This embryo is beginning to undergo cell death as evidenced by the presence of a vacuole. Panels (C) and (D) are immunofluorescent micrographs of embryos stained with mAB-ICB4 an antibody that recognizes intestinal cells (Bowerman et al., 1992). Again, the wild-type embryo (C) has initiated morphogenesis and will ultimately elongate four-fold before hatching. It is clear that the stained cells have been organized into the tissue that will form the intestine. In contrast, the *src-1(cj293)* embryo (D) has failed to initiate morphogenesis and will continue to develop as a disorganized sphere of cells.

Figure 16 - Generation of *C. elegans* founder cells.

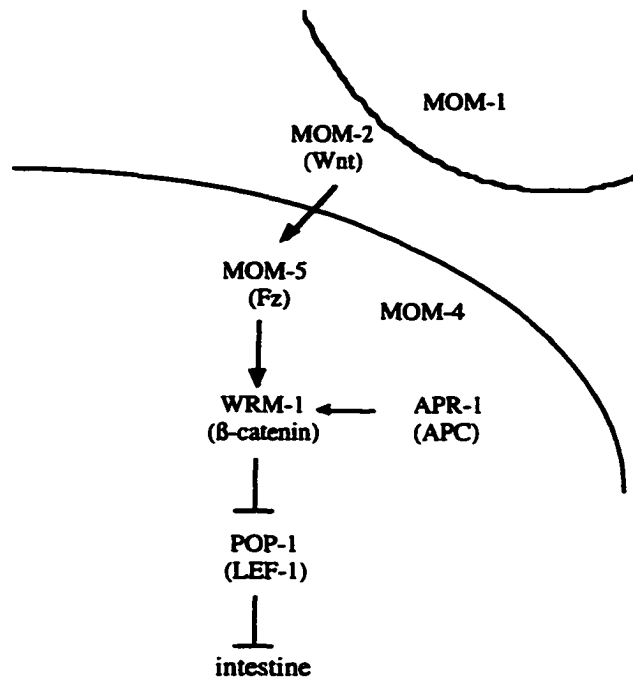


Legend: P₀ is the name given to a fertilized *C. elegans* oocyte. This single cell divides to form the cells designated AB and P₁. The following cell divisions generate six founder cells: AB, MS, E, C, D, and P₄. Each founder cell executes a unique pattern of cell divisions and cell fates to give rise to all of the organisms tissues. The tissues types normally derived from each founder cell are as follows: AB - hypodermis, neurons, muscle; MS - muscle, glands, neurons; E - intestine; C - muscle, hypodermis, neurons; D - muscle; P₄ - germline.

revealed what appear to be extra intestinal cells in approximately 50% of *src-1(cj293)* embryos. While the source of these extra intestinal cells has not been determined (see discussion), their presence suggests that SRC-1 may normally play a role in regulating cell fate decisions of developing embryos.

Recent studies have shown that the Mom pathway (Figure 17), similar to the Wnt signaling pathway of vertebrates and the Wg signaling pathway of *Drosophila*, is necessary to specify the normal intestinal fate of the E lineage (Rocheleau et al., 1997; Thorpe et al., 1997). Through MOM-2 (Wnt/Wg) signaling at the four-cell embryonic stage, P₂ normally polarizes the neighboring EMS blastomere to divide asymmetrically thereby establishing the intestinal fate of its posterior daughter E. MOM-2 signaling appears to mediate this effect by reducing the levels of POP-1, an HMG box protein with homology to vertebrate transcription factors Tcf-1 and Lef-1 and the *Drosophila* transcription factor Pangolin (Lin et al., 1998). Loss-of-function *mom-2*, *mom-4*, *mom-5* (Fz), and *apr-1* (APC) mutants normally exhibit a variably penetrant more mesoderm (Mom) phenotype. That is, they produce more mesoderm and lack intestine due to failure of EMS to divide asymmetrically in the presence of elevated POP-1 levels (Rocheleau et al., 1997; Thorpe et al., 1997). If SRC-1 normally influences cell fate decisions of the E lineage by regulating MOM-2 signaling, then the penetrance of the Mom phenotype for each of these mutants would be expected to be enhanced (if SRC-1 acts as a positive regulator) or suppressed (if SRC-1 acts as a negative regulator) in a *src-1(cj293)* background. To test this hypothesis, my collaborators constructed double mutants using RNA-mediated interference of Mom pathway members *mom-2*, *mom-4*, *mom-5*, and *apr-1* in a *src-1(cj293)* background. We found that the penetrance of the Mom phenotype was enhanced to 100%, or nearly 100%, for all four Mom pathway components tested (Table 6, Figure 18) suggesting that SRC-1 normally regulates MOM-2 signaling in the E lineage in a positive manner. Furthermore, simultaneously disrupting *pop-1* restores intestinal cell production in the triple mutants suggesting that the function of SRC-1, APR-1, and the MOM proteins is to reduce POP-1 levels in the E blastomere.

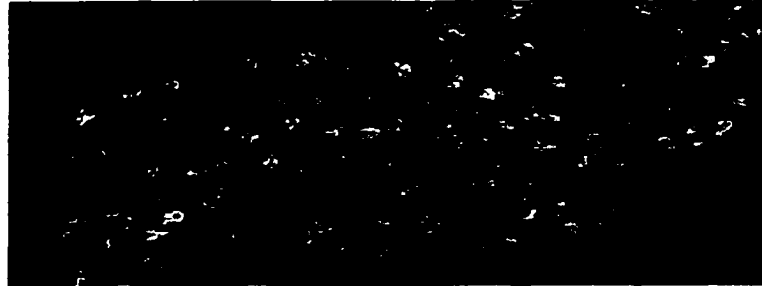
Figure 17 - The *C. elegans* Mom pathway.



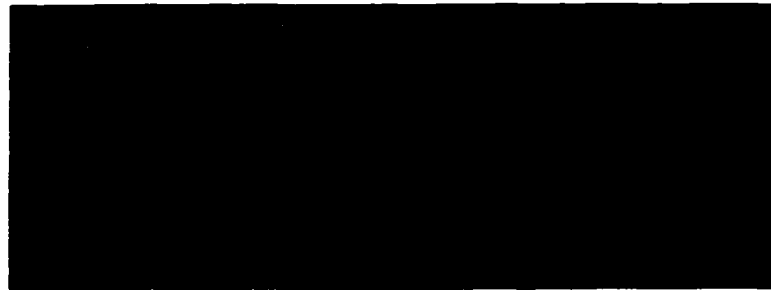
Legend: This figure is based on genetic data reported by both Craig Mello's (Rocheleau et al., 1997) and Bruce Bowerman's (Thorpe et al., 1997) laboratories. MOM-2 signal, secreted from the P₂ blastomere, is believed to be received by the MOM-5 receptor of the neighboring EMS blastomere. Propagation of the signal through WRM-1 leads to down regulation of POP-1 such that POP-1 is no longer able to inhibit intestine formation in the posterior daughter of EMS. By genetic analysis, APR-1 appears to act as a second input that impinges on the pathway upstream of WRM-1. The genetic placement of MOM-4 (a serine/threonine kinase) is unresolved, but it appears to also act upstream of WRM-1 (Rocheleau and Mello, personal communication).

Figure 18 - Genetic analysis of intestine formation in *src-1* mutants.

(A) *mom-5(RNAi)*



(B) *mom-5(RNAi); src-1(cj293)*



Legend: The pictures shown in this figure were taken by Yanxia Bei. Panel (A) depicts a field of *mom-5(RNAi)* embryos viewed under plane-polarized light. Under these conditions, gut granules autofluoresce identifying which embryos have produced intestinal cells. As shown, approximately 95% of *mom-5(RNAi)* embryos produce intestinal cells. Only about 5% exhibit a Mom (more mesoderm) phenotype which is characterized by absence of intestinal cells. Panel (B) depicts a field of *mom-5(RNAi); src-1(cj293)* double mutant embryos also viewed under plane-polarized light. As shown, mutation of *src-1* enhances penetrance of the Mom phenotype to 100% in a *mom-5* mutant background.

Table 6 - Genetic analysis of intestine formation in *src-1* mutants.

Embryo genotype	% Embryos lacking intestine (n)
<i>mom-2(ne141)</i>	66(212)
<i>mom-2(ne141); src-1(RNAi)</i>	99(461)
<i>mom-2(ne141); src-1(RNAi); pop-1(RNAi)</i>	0(64)
<i>mom-2(RNAi)</i>	11(125)
<i>mom-2(RNAi); src-1(cj293)</i>	98(149)
<i>mom-4(ne19)</i>	41(154)
<i>mom-4(ne19); src-1(RNAi)</i>	96(113)
<i>mom-4(ne19); src-1(RNAi); pop-1(RNAi)</i>	0(51)
<i>mom-5(zu193)</i>	4(137)
<i>mom-5(zu193); src-1(RNAi)</i>	100(247)
<i>mom-5(RNAi); src-1(cj293)</i>	100(325)
<i>mom-5(RNAi); src-1(cj293); pop-1(RNAi)</i>	0(31)
<i>apr-1(RNAi)</i>	26(318)
<i>apr-1(RNAi); src-1(cj293)</i>	99(215)
<i>apr-1(RNAi); src-1(cj293); pop-1(RNAi)</i>	0(52)

Note - Data presented in this table was provided by Yanxia Bei.

I wanted to define the molecular basis for the genetic interactions observed between *src-1(cj293)* and the Mom pathway mutants. Specifically, I wanted to determine whether any components of the Mom pathway might interact with SRC-1. As a non-receptor tyrosine kinase it is unlikely that SRC-1 directly receives the MOM-2 signal. Likewise, with no evidence that serpentine class receptors target tyrosine kinases, it seems unlikely that MOM-5 would directly activate or recruit SRC-1. While there is no evidence that Src can affect the Wnt signaling role of β -catenin, evidence from mammalian cell culture suggests that Src may affect the role of β -catenin in cadherin-based cell-cell adhesion (see discussion). If Src can affect one aspect of β -catenin function, it seems likely that it could

also affect the other. Mom pathway component *wrm-1* encodes a *C. elegans* homolog of β -catenin (Rocheleau et al., 1997) making it the best candidate for a target of SRC-1 signaling within the Mom pathway.

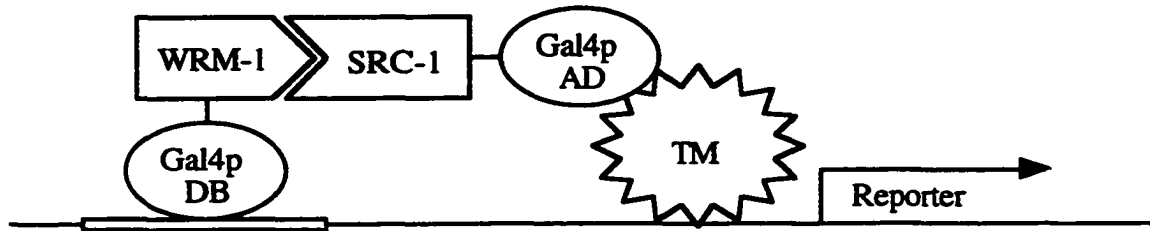
Testing for a Direct Interaction between SRC-1 and WRM-1.

I have used the yeast two-hybrid system to test for a direct interaction between SRC-1 and WRM-1. This technique is based on the premise that transcriptional activators possess two separable domains, a DNA-binding domain and an activation domain which interacts with the transcriptional machinery, both of which are necessary for activation of transcription. While the two domains need to be in close proximity, they do not need to be included in the same protein in order to achieve activation of transcription. I have exploited this fact in order to test whether SRC-1 and WRM-1 interact directly. To this end I subcloned full length *src-1* cDNA into pACT2 (Clonetech), a vector which contains a clone of the activation domain of the transcriptional activator GAL4. Fused SRC-1 is constitutively expressed downstream of, and in frame with, the Gal4p activation domain when this plasmid is transformed into yeast strain HF7c (Clonetech). A plasmid encoding WRM-1 fused to the DNA-binding domain of Gal4p was obtained from the Mello laboratory and co-transformed with the constructed *src-1* fusion plasmid. When expressed, the WRM-1 fusion protein binds Gal4p recognition sequences upstream of the LacZ and HIS3 reporter genes used in this assay. If SRC-1 and WRM-1 physically interact, the Gal4p activation domain fused to SRC-1 will be brought to the region upstream of the reporter genes allowing contact with the transcriptional machinery and resulting in transcription of LacZ and HIS3 (Figure 19). Co-transformation of plasmids encoding the SRC-1 and WRM-1 fusion proteins failed to activate transcription of LacZ or HIS3 above background levels.

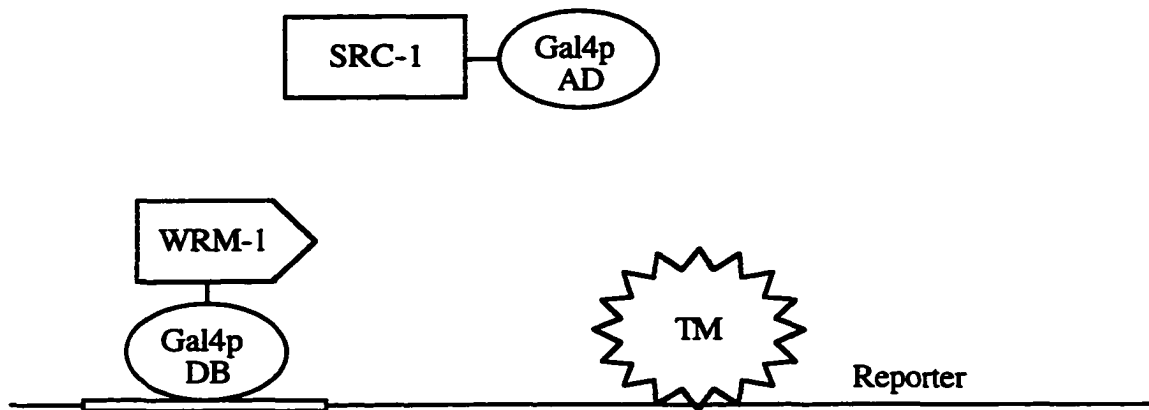
To confirm that the full length SRC-1 fusion protein was being expressed, I analyzed protein extracts prepared from a yeast strain harboring the plasmid by SDS-PAGE. Western blotting with an anti-HA antibody that recognizes the HA epitope tag

Figure 19 - Two-hybrid assay to test for a SRC-1, WRM-1 interaction.

(A)



(B)



Legend: In this system, the Gal4p DNA-binding domain binds to recognition sequences upstream of the reporter gene bringing the fused WRM-1 protein to the DNA. Panel (A) depicts the scenario where SRC-1 and WRM-1 interact. As a result of SRC-1 binding WRM-1, the fused Gal4p activation domain (AD) is physically brought to the DNA where it can interact with the transcriptional machinery (TM) activating transcription of the reporter gene. Panel (B) depicts the opposite scenario where SRC-1 and WRM-1 do not interact. Because SRC-1 does not bind WRM-1, the fused Gal4p activation domain is not recruited to the DNA and is unable to interact with the transcriptional machinery. As a result, the reporter gene is not transcribed.

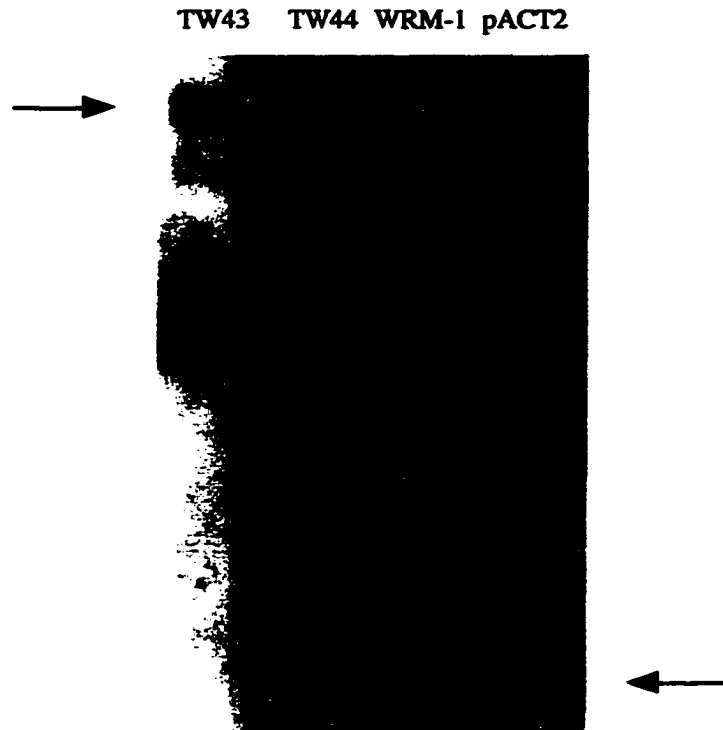
engineered into the Gal4p DNA-binding domain detects a band consistent with the predicted size of the full length SRC-1 fusion protein (Figure 20). Confident that the SRC-1 fusion protein was being expressed, I decided to sequence one of the plasmids to determine if any point mutations had been introduced in the process of subcloning that might render the fusion unable to interact with WRM-1. Nearly complete sequencing of pTW44 *src-1* insert revealed the presence of three point mutations. A mutation within the SH3 domain does not result in an amino acid change and a mutation within the kinase domain results in a conserved amino acid change (Table 7). Neither of these mutations are likely to compromise function of the SRC-1 fusion protein. On the other hand, the third mutation results in an isoleucine to methionine change within the phosphotyrosine binding pocket of the SH2 domain. This change of a highly conserved amino acid could affect an interaction mediated by this domain. Because of this mutation, the results of this two-hybrid analysis are inconclusive at best. In order to determine that the failure of the reporter genes to be activated is not due to this mutation, it would be necessary to make and sequence additional, independent SRC-1 fusion constructs.

Table 7 - Point mutations identified within the *src-1* insert of pTW44.

Mutation	Amino Acid Change	Coding Region Affected
T → C	None	SH3 domain
A → G	Ile → Met	SH2 domain
T → A	Leu → Ile	kinase domain

Despite failing to interact with the Gal4p-WRM-1 fusion protein to activate transcription of the LacZ and HIS3 reporters, I tested whether or not the Gal4p-SRC-1 fusion protein encoded by the pTW44 construct was able to phosphorylate the WRM-1 fusion protein when expressed in yeast. Western blotting protein extracts with an anti-phosphotyrosine antibody (Upstate Biotechnology) as well as immunoprecipitation of yeast

Figure 20 - The Gal4p-SRC-1 fusion is expressed in yeast.



Legend: This figure depicts a western blot of yeast protein extracts using a commercial anti-HA antibody (Santa Cruz). Lanes 1 and 2 contain protein extracts isolated from yeast transformed with pTW43 and pTW44. These plasmids are independent clones of *src-1* fused downstream of the activation domain of GAL4. The size of these bands are consistent with the predicted molecular weight of approximately 75 Kd expected for the fusion protein. Lane 3 contains protein extracts from yeast transformed with a *wrm-1* fusion clone. No protein is detected because the protein is not tagged with the HA epitope. Lane 4 contains protein extracts from yeast transformed with pACT2, the GAL4 activation domain vector into which *src-1* was sub-cloned. The size of the band is consistent with the predicted molecular weight of approximately 15 Kd expected for the activation domain alone.

extracts with the same anti-phosphotyrosine antibody failed to detect tyrosine-phosphorylated Gal4p-WRM-1 in the presence or absence of the SRC-1 fusion protein (data not shown). Based on these experiments it appears that either the conserved leucine to isoleucine substitution in the kinase domain abolishes SRC-1 kinase activity or that WRM-1 is not a target for tyrosine phosphorylation by SRC-1 when expressed in yeast.

Testing for a Genetic Interaction between *src-1(cj293)* and *clr-1(e1745ts)*.

clr-1 encodes a receptor protein-tyrosine phosphatase that interacts genetically with components of a conserved fibroblast growth factor (FGF) signaling pathway that controls migration of sex myoblasts in *C. elegans* (Kokel et al., 1998). *clr-1(e1745ts)* is a temperature-sensitive mutant allele. The strain has a wild-type phenotype when grown at 16°C. However, when shifted to 25°C, the strain exhibits a distinctive clear body (Clr) phenotype and becomes sterile. The Clr phenotype is characterized by fluid filling the pseudocoelom such that organs appear to be floating and cell-cell contacts appear to be disrupted. This phenotype can be mimicked by increased EGL-15 signaling suggesting that this phosphatase normally down regulates signaling through the FGF pathway (Kokel et al., 1998). While characterization of *src-1(cj293)* arrested embryos did not suggest a connection between SRC-1 and the *C. elegans* FGF pathway, previous overexpression studies have suggested that SRC-1 may act on this pathway. Overexpression of either wild-type or unregulated (Y527F) *src-1* constructs results in a Clr-like phenotype similar to that observed in *clr-1(e1745ts)* mutants (Thacker and Capecchi, personal communication). This observation suggests that SRC-1 may normally act as an antagonist to CLR-1 phosphatase activity in the FGF signaling pathway. If this hypothesis is true, perhaps the antagonistic relationship between these two proteins is also important for regulating morphogenesis and / or cell fate decisions during embryogenesis. For this reason, I anticipated that *clr-1(e1745ts)* might be able to suppress the Mel phenotype of *src-1(cj293)* mutants.

To test this hypothesis I used standard genetic crosses to introduce *clr-1(e1745ts)*

into a *src-1(cj293)* background. Mutation of *clr-1* was unable to suppress the maternal effect embryonic lethality of *src-1(cj293)* mutants when shifted to the restrictive temperature (Table 8). Similarly, I saw no evidence that mutation of *src-1* was able to suppress the Clr, sterile phenotype of *clr-1(e1745ts)* mutants (data not shown). However, these results do not preclude the possibility that mutation of *clr-1* may be able to suppress the morphogenesis defects observed in *src-1* mutants or the cell fate defects of *src-1* mutants observed in *mom-2*, *mom-4*, *mom-5*, or *apr-1* mutant backgrounds. Experiments to test these possibilities are being pursued by members of Craig Mello's laboratory.

Table 8 - Genetic analysis of *src-1(cj293); clr-1(e1745ts)* double mutants.

Temperature	Time Beyond Temperature Shift	CLR-1 Activity	% Embryos Hatched (n)
16°C	-----	+	0(503)
25°C	0-6 hrs.	-	0(127)
25°C	6-30 hrs.	-	0(117)

DISCUSSION

The goal of my dissertation was to determine the biological role of the *C. elegans* Src ortholog, *src-1*. I addressed this problem using a combination of molecular genetic and biochemical approaches. This study is based on the assumption that the nematode protein has the same function as, and is regulated in the same manner as, its vertebrate homolog pp60^{C-SRC}. In support of this hypothesis, I have shown that wild-type SRC-1 protein is tyrosine phosphorylated in the same manner as pp60^{C-SRC}. To elucidate the biological role of SRC-1, I isolated a loss-of-function mutation in the *src-1* gene using a reverse genetic approach. The embryonic arrest phenotype of this mutant and its ability to interact genetically with components of a Wnt-related pathway suggest that SRC-1 functions through a Wnt signaling pathway to direct morphogenesis and cell fate decisions in the early *C. elegans* embryo. This unexpected result provides the first direct evidence for a connection between two intensively investigated vertebrate signaling pathways: Src and Wnt. As further details of this connection are elucidated, they will shed light on the conserved biological role of each of these developmentally important pathways. Ultimately, such analyses may provide insight into the connections between the normal developmental roles of Src and Wnt signaling and their roles in cancer.

src-1 encodes a pp60^{C-SRC} ortholog.

The *C. elegans src-1* gene encodes a protein with all of the hallmarks of a pp60^{C-SRC} ortholog. All functional domains and individual amino acids critical for localization, protein-protein interactions, and tyrosine kinase activity and regulation are conserved between the nematode and vertebrate proteins. In the vertebrate protein, tyrosine residues 416 and 527 (tyrosine 528 in SRC-1) act as key regulatory points, serving as targets of

phosphorylation. Biochemical studies (Cartwright et al., 1987; Kmiecik and Shalloway, 1987; Piwnica-Worms et al., 1987) and the X-ray crystal structure of c-Src (Superti-Furga and Gonfloni, 1997) and Src-family members Hck (Sicheri et al., 1997) and Lck (Yamaguchi and Hendrickson, 1996) has determined that phosphorylation of tyrosine 527 promotes an interaction between the tail and the SH2 domain maintaining the protein in an inactive conformation. When pp60^{c-src} is activated, the tail becomes displaced, dephosphorylated, and the protein assumes an active conformation that is characterized by phosphorylation of tyrosine 416. Immunoblot analysis of wild-type *C. elegans* extracts using an antibody specific for tyrosine 416 phosphorylated SRC-1 showed that the nematode protein is subject to phosphorylation on this residue. This result demonstrates that at least a fraction of SRC-1 normally exists in a state of phosphorylation associated with catalytically active pp60^{c-src}, providing further evidence that pp60^{c-src} and SRC-1 likely share similar mechanisms of post-translational regulation and function in conserved signaling pathways.

Maternal expression of *src-1* is essential, but zygotic expression is not.

SRC-1 signaling is essential for nematode viability as evidenced by the fully penetrant Mel phenotype of *src-1(cj293)* and *src-1(RNAi)* embryos. This result represents the first example in any system of an essential role for a Src-related protein. All nine vertebrate Src-family members have been knocked-out in mice, with little affect. In each case the mutant mice exhibit only restrictive phenotypes at best, even when widely expressed Src-family kinases like c-Src, Fyn, and c-Yes are disrupted (reviewed in Lowell and Soriano, 1996). Directed overexpression of a dominant-negative form of Dsrc41, the closest c-Src relative found so far in *Drosophila*, results in defective eye morphogenesis, suggesting that it may play an essential role in ommatidial development (Takahashi et al., 1996). However, this theory remains to be tested by isolation of a Dsrc41 mutant. More recently, mutations in a second *Drosophila* Src homolog, Dsrc64, have been isolated.

Dsrc64 mutant flies are viable and develop normally; the only apparent phenotypic consequence is reduced female fertility, apparently due to defects in ring canal morphogenesis (Dodson et al., 1998). These results suggest that functional redundancy between closely related proteins will compromise genetic analysis of Src function in *Drosophila* as well.

I was not surprised to find a maternal requirement for *src-1*. Northern analysis and immunofluorescence studies show that *src-1* is maternally supplied in wild-type animals (Thacker and Capecchi, personal communication). Similarly, transcripts which likely represent maternal message have been identified for one of the *Drosophila* Src homologs (Simon et al., 1985). I do find it curious that no zygotic phenotype is observed. While the range of phenotypes seen in zygotically rescued heterozygotes suggest that SRC-1 may have additional roles beyond its essential role in embryogenesis, these phenotypes are never seen in *src-1(cj293)* homozygotes born from heterozygous mothers. One explanation for the apparent lack of zygotic phenotype could be the presence of a protein transcribed from truncated *src-1(cj293)* message. While such a protein would lack kinase activity, it is in theory possible to argue for a kinase-independent role that is met by the potentially intact unique and/or SH3 domain. I consider such an explanation unlikely because the identical nature of the *src-1(cj293)* and *src-1(RNAi)* phenotypes suggests that even if present, the truncated protein does not supply this function.

A second, more likely explanation for the absence of a zygotic phenotype could be redundancy with one or more additional Src-related kinases. In support of this explanation, one other Src-like gene, F49B2.5, has been identified within the nearly complete *C. elegans* genome sequence. SRC-1 shares 40% overall sequence identity with F49B2.5. Sequence conservation is highest (52% identity) across the kinase domains of these proteins (Figure 21). Disruption of F49B2.5 by RNAi fails to produce a phenotype (Bei and Mello, personal communication). This could be due to failure of the technique, but it is also consistent with the idea that F49B2.5 may function redundantly with SRC-1. This redundancy would be limited to the zygotic function of these proteins as SRC-1 has an essential maternal function evidenced by the Mel phenotype. Isolation of an F49B2.5

Figure 21 - Alignment of *C. elegans* SRC-1 and F49B2.5 kinase domains.

```
QQNWEIPRNQLHLKRKLGDGNFGEVWY GKWRGIVEVAIKTMKPGTMS
:::| | : | : : | | : : | | | | | | | | | | | | | | | | |
DDQWEVDRRSVRLIRQIGAGQFGEVWEGRWNVNVPVAVKKL KAGTAD
```

```
PEAFLLQEAQIMKQC DHPNLVKLYAVCTREEPFYIITEYMINGSLLQY
|.|||.||||| | | : | | : | | | | | | | | | | | | | | | | |
PTDFLAEAQIMKKLRHPKLLSLYAVCTRDEPILIVTE-LMQENLLTF
```

```
LRTD GSTLG I QALVDMAAQIANGMMYLEERKLVHRDLAARNVLVGDK
| : | . : : . | : : | | : | . | | | | | | | | | | | | | | | |
LQRGRQC QMPQLVEISAQVAAGMAYLEEMNF IHRDLAARNILINNS
```

```
ISGV P VVKVAD FGLARKLMEEDI YEARTGAKFP IKWTAPEAATCGNC
: | . . | | : | | | | | | | | | | | | | | | | | | | | | . . .
LS-----VKIADFGLARILMKENEYEARTGARFP IKWTAPEAANYNRF
```

```
TVKSDVWSY G ILLYEIMTKGQVPYPGMHNREVVEQVELGYRMPMPRG
|.||||||| : | | | | | | | | | : | : : | | | | | | | | | | |
TTKSDVWSFGILLTEIVTFGRLPYPGMTNAEVLQQVDAGYRMPCPAG
```

```
CPEQIYEEVLLKCDKTPDRRPTFDTL SRC-1
| | : | : : : | | . . | | : | | | | | | | | | | | |
CPVTLVD-IMQQCWRS DPDKRPTFETL F49B2.5
```

Legend: SRC-1 has 52% identity to F49B2.5 over the kinase domain. Identities are indicated by dashes and similarities are indicated by dots.

knock-out allele is needed to verify the lack of phenotype.

In contrast, this gene appears to encode a uniquely divergent Src-related kinase. The predicted protein encoded by F49B2.5 contains all structural domains and conserved residues characteristic of Src-family kinases with one critical exception. The phosphotyrosine binding pocket of the SH2 domain, called the FLVRES region, is deleted (Figure 22). Mutation of amino acids in this highly conserved region of pp60^{c-Src} have been shown to disrupt protein-protein interactions via the SH2 domain (Hidaka et al., 1991). Absence of the FLVRES region within F49B2.5 would likely affect selection and binding of substrates as well as regulation by the C-terminal tail suggesting that F49B2.5 may function very differently from c-Src and SRC-1.

In addition to F49B2.5, other more distantly related kinases, including a putative Abelson tyrosine kinase ortholog *abl-1* (Goddard et al., 1986), have been identified. Of the vertebrate Src superfamilies Abl, Btk, and Csk, the Abl family shares the greatest sequence identity with Src-family members over the SH3, SH2, and kinase domains and thus may share the greatest potential for functional overlap (reviewed in Superti-Furga and Courtneidge, 1995). Consistent with the idea of functional redundancy between Abl- and Src-related tyrosine kinases, the mouse *disabled* homolog has been shown to physically interact with both full length Abl and the c-Src SH2 domain *in vitro* (Howell et al., 1997). The ability to address the issue of functional overlap between ABL-1 and SRC-1 awaits isolation of an *abl-1* loss-of-function allele.

SRC-1 regulates morphogenesis and cell fate decisions of developing embryos.

Examination of *src-1(cj293)* arrested embryos identified defects in morphogenesis and regulation of cell fate decisions. During *C. elegans* embryogenesis, hypodermal cells are involved in two processes, enclosure and elongation. These events transform the initially spherical mass of embryonic cells into a thin worm that increases approximately four-fold in length before hatching (Sulston et al., 1983; Priess and Hirsh, 1986; Williams-Masson et al., 1997). Morphogenesis begins as hypodermal cells born on the dorsal

Figure 22 - Alignment of *C. elegans* SRC-1 and F49B2.5 SH2 domains.

```
WYAGKIPRNRAERLVLSSHLPKGTFLIREREADTREFAL̄TIRDTDDQRNG
.:.:.:.:.:.:.:.:.:.:.:.:.:.:.:.:.:.:.:.:.:.:.:.:.:.:.:.:.:
IFFSFVTFQKLSKKKQTHQIP--SFL-----KFEDCIR-----EN

GTVKHYKIKRLDHDQGYFITTRRTFRSLQELVRYSDVPDGLCRQLTFPA SRC-1
.:|:|:|:|:|:|:|:|:|:|:|:|:|:|:|:|:|:|:|:|:|:|:|:|:|:|:|:|:|
DSVKHYRIRQLDHG-GYFIARRRPFATLHDLIAHYQREADGLCVNLGAPC F49B2.5
```

Legend: SRC-1 has 38% identity to F49B2.5 over the SH2 domain. The FLVRES binding pocket is boxed. Identities are indicated by dashes and similarities are indicated by dots.

surface of the embryo develop adherens junctions and begin to spread as a sheet across the embryo until the edges of the sheet meet at the ventral midline (Williams-Masson et al., 1997). Once enclosure has been achieved, the cytoskeleton of the hypodermal cells reorganizes (Priess and Hirsh, 1986; Costa et al., 1997), the cells begin to change shape, and the body elongates (Sulston et al., 1983; Priess and Hirsh, 1986).

The morphogenesis defect of *src-1(cj293)* mutants appears to be due to failure of hypodermal cells to enclose the embryo. Three recently described genes *hmp-1*, *hmp-2*, and *hmr-1* have each been shown to be required for proper migration of hypodermal cells during body enclosure and for proper body elongation (Costa et al., 1998). These genes encode proteins related to α -catenin, β -catenin, and cadherin respectively which localize to adherens junctions on the inner membrane of hypodermal cells providing evidence for the role of a catenin-cadherin system in morphogenesis of *C. elegans* embryos. Src-family kinases have been localized to adherens junctions in vertebrate cell lines, where they may act to regulate assembled catenin-cadherin complexes (Tsukita et al., 1991). Several studies have shown that expression of *v-src* leads to increased tyrosine phosphorylation of cadherin-associated β -catenin and decreased cell-cell adhesion (Matsuyoshi et al., 1992; Behrens et al., 1993; Hamaguchi et al., 1993). Based on these observations, it seems plausible that SRC-1 may normally act in the adherens junctions of hypodermal cells to regulate a HMP-1, HMP-2, HMR-1 complex which controls morphogenesis in developing *C. elegans* embryos. Loss of SRC-1 kinase activity may destabilize this complex such that appropriate cell-cell connections are not made leading to the morphogenesis defect observed in *src-1(cj293)* mutants. This model could be tested in the future by generating double mutants of *src-1(cj293)* and *hmp-1*, *hmp-2*, and *hmr-1* mutants. If SRC-1 normally signals through any of these proteins to promote hypodermal enclosure and / or elongation, *src-1(cj293)* may be expected to enhance the morphogenesis defect of these zygotic lethal mutants. That is, enclosure and elongation defects of *hmp-1*, *hmp-2*, and *hmr-1* mutants may become more severe in a *src-1(cj293)* background. Additionally, biochemical analyses could be used to test directly for a physical interaction between SRC-1 and each of the members of the catenin-cadherin complex. Alternatively, SRC-1 may only affect

morphogenesis indirectly by regulating cell fate decisions that normally produce hypodermal cells involved in enclosure and elongation.

Examination of *src-1(cj293)* arrested embryos uncovered evidence of inappropriate cell fate decisions. My collaborators in the Mello laboratory found that many arrested *src-1* mutant embryos contained 30 intestinal cells. Wild-type embryos always produce 20 intestinal cells, all of which are derived from a single founder cell, the E blastomere. The extra intestinal cells in *src-1(cj293)* embryos do not appear to result from excess proliferation of the E lineage. Because all intestinal cells of *src-1(cj293)* embryos appear to be of normal size, it seems most likely that another blastomere lineage is inappropriately producing the intestinal cells at the expense of a different cell type. To determine the source of these extra intestinal cells, we used laser ablation analysis. When the E blastomere is ablated, the arrested *src-1* embryos fail to make any intestinal cells suggesting that the E blastomere is the source of the extra intestinal cells. This result is in conflict with the observation that all 30 intestinal cells of *src-1(cj293)* embryos are of normal size. One model consistent with all of the data is that the extra intestinal cells do not arise from the E lineage, but depend upon either the E blastomere or its descendants to produce intestinal cells. Perhaps the fate of the extra cells is sensitive to the timing of ablation of the E blastomere such that they only develop if the E blastomere or its descendants are present at some critical time point. Additional ablation experiments where descendants of the E blastomere are ablated at time points later in development should resolve this issue.

Regardless of the source of the extra intestinal cells, *src-1(cj293)* clearly influences cell fate decisions in *mom-2*, *mom-4*, *mom-5*, and *apr-1* mutant backgrounds. Eliminating SRC-1 kinase activity enhances the Mom phenotype of all four mutants such that in 100% of double mutant embryos the E blastomere incorrectly adopts an MS-like fate. The fact that *src-1(cj293)* interacts genetically with these mutants suggests that SRC-1 may normally affect cell fate decisions in the E blastomere lineage by regulating signaling through this Wnt-related pathway. Because mutation of *src-1* on its own has no effect on cell fate decisions of the E lineage, it is probably not an obligate member of the Mom pathway. However, since mutation of *src-1* enhances penetrance of the Mom phenotype to

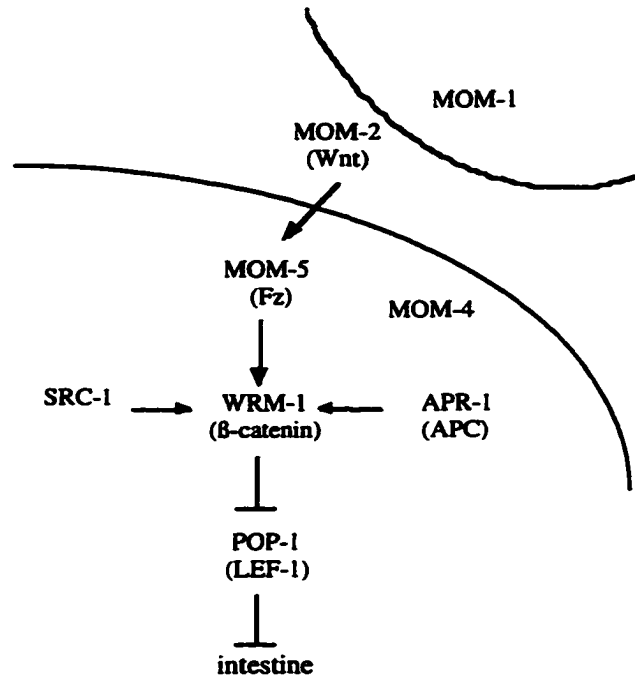
100% for all of the *mom* genes and *apr-1*, it appears that *src-1* likely feeds into the Mom pathway downstream of these components. The fact that mutation of *pop-1* completely suppresses the Mom phenotype of *src-1* double mutants suggests that *src-1* acts upstream of *pop-1*. Still unresolved is at which component SRC-1 may be exerting its affect on the Wnt pathway.

Unlike the model described for the morphogenesis defect, vertebrate studies provide little insight into how SRC-1 may normally regulate such a pathway. In fact, the only information that sheds any light on this question comes from the study discussed above which showed that expression of *v-src* leads to increased tyrosine phosphorylation of cadherin-associated β -catenin (Matsuyoshi et al., 1992; Behrens et al., 1993; Hamaguchi et al., 1993). In addition to its role in cell-cell adhesion, β -catenin also plays a role in Wnt signaling that is independent of cadherin. Studies using vertebrate cell lines have shown that Wnt-1 signaling stabilizes an unassociated pool of β -catenin which results in propagation of the Wnt-1 signal (Hinck et al., 1994; Papkoff et al., 1996; Papkoff, 1997). This population of β -catenin also becomes tyrosine phosphorylated when *v-src* is expressed (Papkoff, 1997). While tyrosine phosphorylation does not result in an apparent stabilization of this unassociated β -catenin pool, perhaps it affects the activity of β -catenin in a different manner that also results in propagation of the Wnt-1 signal. This would suggest that SRC-1 may normally affect cell fate decisions by acting to regulate MOM-2 signaling through phosphorylation of WRM-1, another *C. elegans* homolog of β -catenin (see Figure 23). I have used a directed two-hybrid approach to test this hypothesis.

Directed two-hybrid analysis fails to detect, but does not rule out, an interaction between SRC-1 and WRM-1.

Using the yeast two-hybrid system, I tested whether SRC-1 and WRM-1 can interact directly *in vivo*. Similar analyses have been used successfully to detect an interaction between vertebrate Src-family kinase members and putative targets even where the interaction is mediated by binding of the Src-family kinase SH2 domain to a

Figure 23 - A genetic model for SRC-1 function in regulating the intestinal cell fate decision.



Legend: Genetic analysis of *src-1* loss-of-function mutants is consistent with SRC-1 acting downstream of, or in parallel to the MOM proteins and APR-1, but upstream of POP-1. Based on the genetic placement of *src-1*, and the known properties of vertebrate pp60^{c-src} and β-catenin, WRM-1 appears to be a likely target of SRC-1 tyrosine kinase activity.

phosphorylated tyrosine residue of the target protein (Dombrosky-Ferlan and Corey, 1997). While such post-translational modifications are not endogenous to yeast, expression of a catalytically active Src-family kinase in the same cell can lead to tyrosine phosphorylation of the target protein. Based on this study, I anticipated that if SRC-1 normally phosphorylates WRM-1, then a directed two-hybrid experiment would detect an interaction.

Expressing the appropriate SRC-1 and WRM-1 fusions in yeast did not detect such an interaction. This result suggests that the two proteins can not interact directly. However, DNA sequence analysis of the *src-1* vector has brought into question the inherent ability of the fusion protein to participate in protein-protein interactions. A point mutation identified within the phosphotyrosine binding pocket of the SH2 domain could be expected to disrupt any protein-protein interactions mediated by this domain thereby explaining why SRC-1 and WRM-1 failed to interact in this assay. Additionally, the SRC-1 fusion is unable to phosphorylate WRM-1 in yeast suggesting that the conserved amino acid substitution in the kinase domain may impair catalytic activity of the protein. Constructing additional, independent *src-1* fusion clones would resolve the question of functional integrity introduced by these mutations. If an interaction can be detected with a wild-type clone, this existing "mutant" clone will have identified a residue or residues important for interaction between SRC-1 and WRM-1. Additionally, other biochemical approaches such as coimmunoprecipitation from *C. elegans* extracts could be employed that would avoid the problem of introducing mutations via subcloning.

Alternatively, SRC-1 may normally act on WRM-1 indirectly through an intermediate or another protein complexed with WRM-1. Vertebrate proteins APC (adenomatous polyposis coli) and GSK-3 (glycogen synthase kinase) have been shown to form a complex with β -catenin in tumor cell lines expressing truncated forms of APC protein (Rubinfeld et al., 1996). A current model derived from this and other studies suggests that in the absence of Wnt signaling GSK-3 and APC normally work in concert to promote degradation of cytoplasmic fractions of β -catenin (reviewed in Cadigan and Nusse, 1997). By this model Wnt signaling antagonizes GSK-3 and APC activity thereby

stabilizing β -catenin. As a result, β -catenin can be translocated to the nucleus where it interacts with downstream transcription factors. *sgk-1* (Bei and Mello, personal communication) and *apr-1* (Rocheleau et al., 1997) have recently been shown to encode *C. elegans* homologs of GSK-3 and APC respectively. Although genetic analysis places these genes in slightly different positions within the conserved Wnt pathway than those described for their vertebrate and *Drosophila* counterparts, it seems likely that the proteins may form a complex with WRM-1. If so, both would be obvious candidates for intermediates that act between SRC-1 and WRM-1.

I must also consider the possibility that SRC-1 does not act on any component of the Mom pathway, and likewise, related tyrosine kinases do not act on the Wg pathway of *Drosophila* or the Wnt pathway of vertebrates. The genetic interactions observed with *src-1(cj293)* are consistent with it acting downstream of, or in parallel to, *mom-2*, *mom-4*, *mom-5*, and *apr-1* and acting upstream of *pop-1*. It is therefore possible that SRC-1 acts only in an independent parallel pathway which also regulates cell fate decisions through antagonizing POP-1. Additional genetic analyses of the *src-1(cj293)* allele in combination with biochemical analyses to characterize SRC-1 protein-protein interactions will be needed to distinguish among these and other scenarios.

SRC-1 may be important for defining anterior-posterior polarity of asymmetric cell divisions.

To this point, I have focused only on involvement of POP-1 in specification of the intestinal cell fate. As described, reducing POP-1 levels by activation of the Mom pathway results in the E lineage assuming an intestinal cell fate (Lin et al., 1998). However, POP-1 appears to have a broader role in specifying anterior fates throughout the embryo. Recall that at the four-cell stage of embryogenesis, MOM-2 signaling by the P2 blastomere polarizes the EMS blastomere to divide asymmetrically. The posterior daughter E does not contain POP-1 and ultimately adopts an intestinal cell fate. The anterior daughter MS does contain POP-1 and ultimately adopts a mesoderm fate. Similarly throughout embryonic

development, the anterior daughters of asymmetric cell divisions accumulate POP-1 and the posterior daughters do not establishing different fates (Lin et al., 1998). Therefore, the presence or absence of POP-1 appears to specify an anterior or posterior fate respectively. This global asymmetric distribution of POP-1 is dependent on WRM-1 activity (Lin et al., 1998). Asymmetric distribution of POP-1 also seems to be dependent on Wnt signaling pathways even though there does not appear to be one universal pathway with global effects. The MOM-2 pathway appears to specifically direct POP-1 asymmetry in the MS and E lineages while activation of LIN-17 (another *C. elegans* homolog of *Drosophila* Frizzled) appears to direct POP-1 asymmetry in seam cells of the male tail (Lin et al., 1998).

Given that Wnt pathways seem to be important for establishing anterior-posterior polarity of asymmetric cell divisions, and that *src-1(cj293)* interacts genetically with multiple Wnt pathway components, it seems possible that SRC-1 may normally play a role in this global process as well. Additional analyses of *src-1(cj293)* arrested embryos are needed to determine if anterior-posterior decisions are affected in any cell lineages. These analyses should include looking for evidence of duplicated anterior cell fates (this is based on the observation that the E blastomere adopts the fate of its anterior sister MS in *src-1(cj293)* double mutant backgrounds) and looking for evidence of POP-1 mislocalization.

SRC-1 regulates cytoskeletal organization in concert with the MOM proteins, but does so independently of WRM-1 and POP-1.

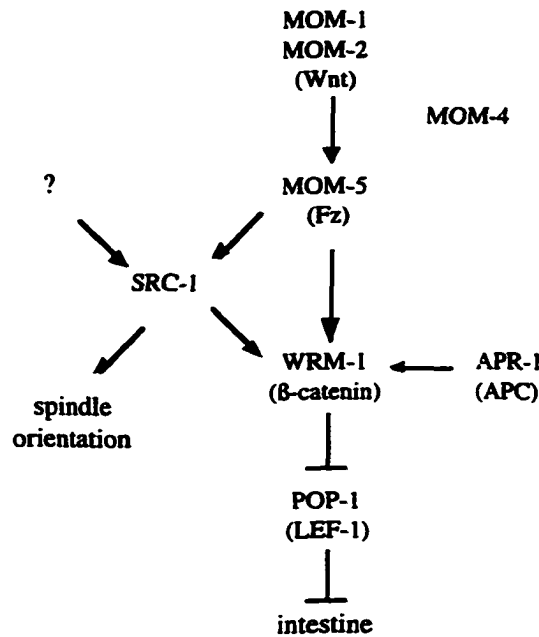
A third defect of *src-1(cj293)* embryos is disrupted mitotic spindle orientation. At the eight-cell stage of embryogenesis, there are four descendants of the AB blastomere: ABpl, ABpr, ABal, and ABar. The mitotic spindles of three of these cells are oriented approximately in parallel to each other. The mitotic spindle of the fourth cell, ABar, is normally oriented perpendicularly to the others. In *src-1(cj293)* embryos, the orientation of the ABar spindle is parallel to the spindles of the other AB descendants. This specific defect is also caused by mutation of the *mom* genes, but is not observed in *wrm-1* or *pop-1*

mutants (Rocheleau et al., 1997) suggesting that SRC-1 and the MOM proteins regulate cytoskeletal organization in a manner that is independent of WRM-1 and POP-1 activity. In contrast to the effects on cell fate decisions, this effect on spindle orientation appears to be independent of transcriptional activity in general as disruption of *ama-1*, a gene encoding the large subunit of RNA polymerase, does not result in disruption of cleavage axes in any cells until at least the 26-cell stage of embryogenesis (Powell-Coffman et al., 1996). Taken together these results suggest that the Mom pathway branches to meet two separate roles (see Figure 24). One branch signals through WRM-1 to decrease POP-1 levels and direct cell fate decisions of the MS and E blastomere lineages presumably by activating transcription of downstream targets. As previously discussed, SRC-1 is not likely to be an obligate component of the pathway, but likely feeds into the pathway downstream of the *mom* genes and *apr-1*. The other branch targets as yet unidentified proteins which direct mitotic spindle orientation. Because mutation of *src-1* by itself generates the same spindle orientation defect as the *mom* genes, it is likely to be an obligate component of this branch of the pathway.

Mutation of the CLR-1 phosphatase is unable to suppress the Mel phenotype of *src-1* mutants.

Mutation of *clr-1*, a gene that encodes a receptor protein-tyrosine phosphatase (Kokel et al., 1998), fails to suppress the maternal effect embryonic lethality of *src-1(cj293)* mutants. This result is not surprising since I have identified, in collaboration with the Mello laboratory, a potential role for SRC-1 in multiple aspects of embryogenesis including regulation of spindle orientation, morphogenesis, and cell fate decisions. Even if SRC-1 and CLR-1 do normally interact, they may do so only in a subset of SRC-1-regulated processes. Examination of the cellular phenotype of *src-1(cj293); clr-1(e1745ts)* double mutants may reveal that mutation of *clr-1* suppresses one or more of the cellular defects normally observed in *src-1* mutants.

Figure 24 - A genetic model for the separable functions of SRC-1 and the MOM proteins in regulating spindle orientation and the intestinal cell fate decision.



Legend: SRC-1 is unlikely to be an obligate member of the Mom pathway branch that regulates the intestinal cell fate decision. This is based on the observation that *src-1* mutants on their own do not affect intestine formation. It is only in combination with mutation of other Mom pathway members that mutation of *src-1* exerts an effect on this process. On the other hand, SRC-1 appears to be an obligate member of the Mom pathway branch that regulates spindle orientation. Mutation of *src-1* disrupts orientation of the ABar blastomere spindle in the same manner as the *mom* mutants.

In summary, my analysis of a *C. elegans src-1* loss-of-function allele has provided evidence for a connection between two intensively investigated vertebrate signaling pathways: Src and Wnt. The fact that Src and Wnt signaling affect the same developmental processes in *C. elegans* suggests that there may be crosstalk between these two pathways in higher organisms. This study lays the groundwork for further investigations that will contribute to our understanding of the role each of these pathways plays, both in normal vertebrate development and in establishment and progression of cancer, a disease that is in some cases associated with unregulated signaling by Src or Wnt.

REFERENCES

- Appleby, M. W., Gross, J. A., Cooke, M. P., Levin, S. D., Qian, X., and Perlmutter, R. M. (1992). Defective T cell receptor signaling in mice lacking the thymic isoform of p59fyn. *Cell* 70, 751-63.
- Behrens, J., Vakaet, L., Friis, R., Winterhager, E., Van Roy, F., Mareel, M. M., and Birchmeier, W. (1993). Loss of epithelial differentiation and gain of invasiveness correlates with tyrosine phosphorylation of the E-cadherin/beta-catenin complex in cells transformed with a temperature-sensitive v-SRC gene. *J Cell Biol* 120, 757-66.
- Bowerman, B., Tax, F. E., Thomas, J. H., and Priess, J. R. (1992). Cell interactions involved in development of the bilaterally symmetrical intestinal valve cells during embryogenesis in *Caenorhabditis elegans*. *Development* 116, 1113-22.
- Brundage, L., Avery, L., Katz, A., Kim, U. J., Mendel, J. E., Sternberg, P. W., and Simon, M. I. (1996). Mutations in a *C. elegans* Gqalpha gene disrupt movement, egg laying, and viability. *Neuron* 16, 999-1009.
- Burdine, R. D., Chen, E. B., Kwok, S. F., and Stern, M. J. (1997). egl-17 encodes an invertebrate fibroblast growth factor family member required specifically for sex myoblast migration in *Caenorhabditis elegans*. *Proc Natl Acad Sci U S A* 94, 2433-7.
- Cadigan, K. M., and Nusse, R. (1997). Wnt signaling: a common theme in animal development. *Genes Dev* 11, 3286-305.
- Cao, X., Tay, A., Guy, G. R., and Tan, Y. H. (1996). Activation and association of Stat3 with Src in v-Src-transformed cell lines. *Mol Cell Biol* 16, 1595-603.
- Cartwright, C. A., Eckhart, W., Simon, S., and Kaplan, P. L. (1987). Cell transformation by pp60c-src mutated in the carboxy-terminal regulatory domain. *Cell* 49, 83-91.
- Cartwright, C. A., Coad, C. A., and Egbert, B. M. (1994). Elevated c-Src tyrosine kinase activity in premalignant epithelia of ulcerative colitis. *J Clin Invest* 93, 509-15.
- Cobb, B. S., Schaller, M. D., Leu, T. H., and Parsons, J. T. (1994). Stable association of pp60src and pp59fyn with the focal adhesion-associated protein tyrosine kinase, pp125FAK. *Mol Cell Biol* 14, 147-55.
- Collins, J. J., and Anderson, P. (1994). The Tc5 family of transposable elements in *Caenorhabditis elegans*. *Genetics* 137, 771-81.
- Costa, M., Draper, B. W., and Priess, J. R. (1997). The role of actin filaments in patterning the *Caenorhabditis elegans* cuticle. *Dev Biol* 184, 373-84.
- Costa, M., Raich, W., Agbunag, C., Leung, B., Hardin, J., and Priess, J. R. (1998). A

- putative catenin-cadherin system mediates morphogenesis of the *Caenorhabditis elegans* embryo. *J Cell Biol* 141, 297-308.
- DeStasio, E., Lephoto, C., Azuma, L., Holst, C., Stanislaus, D., and Uttam, J. (1997). Characterization of revertants of *unc-93(e1500)* in *Caenorhabditis elegans* induced by N-ethyl-N-nitrosourea. *Genetics* 147, 597-608.
- Dodson, G. S., Guarnieri, D. J., and Simon, M. A. (1998). Src64 is required for ovarian ring canal morphogenesis during *Drosophila* oogenesis. *Development* 125, 2883-92.
- Dombrosky-Ferlan, P. M., and Corey, S. J. (1997). Yeast two-hybrid in vivo association of the Src kinase Lyn with the proto-oncogene product Cbl but not with the p85 subunit of PI 3-kinase. *Oncogene* 14, 2019-24.
- Ferrel, J. E. and Martin, G. S. (1978). Thrombin stimulates the activities of multiple previously unidentified protein kinases in platelets. *J. Biol. Chem.* 264, 20723-29.
- Fodor, A., and Deak, P. (1982). Isolation and phenocritical period-analysis of conditional and non-conditional developmental mutants in *C. elegans*. *Acta Biologica Academiae Scientiarum Hungaricae* 32, 229-239.
- Fukui, Y., Saltiel, A. R., and Hanafusa, H. (1991). Phosphatidylinositol-3 kinase is activated in *v-src*, *v-yes*, and *v-fps* transformed chicken embryo fibroblasts. *Oncogene* 6, 407-11.
- Fumagalli, S., Totty, N. F., Hsuan, J. J., and Courtneidge, S. A. (1994). A target for Src in mitosis. *Nature* 368, 871-4.
- Goddard, J. M., Weiland, J. J., and Capecchi, M. R. (1986). Isolation and characterization of *Caenorhabditis elegans* DNA sequences homologous to the *v-abl* oncogene. *Proc Natl Acad Sci U S A* 83, 2172-6.
- Gould, K. L. and Hunter, T. (1988). Platelet-derived growth factor induces multisite phosphorylation of pp60c-src and increases its protein-tyrosine kinase activity. *Mol. Cell Biol.* 8, 3345-56.
- Grant, S. G., O'Dell, T. J., Karl, K. A., Stein, P. L., Soriano, P., and Kandel, E. R. (1992). Impaired long-term potentiation, spatial learning, and hippocampal development in *fyn* mutant mice. *Science* 258, 1903-10.
- Guedes, S., and Priess, J. R. (1997). The *C. elegans* MEX-1 protein is present in germline blastomeres and is a P granule component. *Development* 124, 731-9.
- Guo, S., and Kemphues, K. J. (1995). *par-1*, a gene required for establishing polarity in *C. elegans* embryos, encodes a putative Ser/Thr kinase that is asymmetrically distributed. *Cell* 81, 611-20.
- Guo, S., and Kemphues, K. J. (1996). Molecular genetics of asymmetric cleavage in the early *Caenorhabditis elegans* embryo. *Curr Opin Genet Dev* 6, 408-15.
- Gupta, S. K., Gallego, C., Johnson, G. L., and Heasley, L. E. (1992). MAP kinase is

- constitutively activated in *gip2* and *src* transformed rat 1a fibroblasts. *J Biol Chem* 267, 7987-90.
- Hamaguchi, M., Matsuyoshi, N., Ohnishi, Y., Gotoh, B., Takeichi, M., and Nagai, Y. (1993). p60^{v-src} causes tyrosine phosphorylation and inactivation of the N-cadherin-catenin cell adhesion system. *Embo J* 12, 307-14.
- Hidaka, M., Homma, Y., and Takenawa, T. (1991). Highly conserved eight amino acid sequence in SH2 is important for recognition of phosphotyrosine site. *Biochem Biophys Res Commun* 180, 1490-7.
- Hinck, L., Nelson, W. J., and Papkoff, J. (1994). Wnt-1 modulates cell-cell adhesion in mammalian cells by stabilizing beta-catenin binding to the cell adhesion protein cadherin. *J Cell Biol* 124, 729-41.
- Hodgkin, J., Papp, A., Pulak, R., Ambros, V., and Anderson, P. (1989). A new kind of informational suppression in the nematode *Caenorhabditis elegans*. *Genetics* 123, 301-13.
- Howell, B. W., Gertler, F. B., and Cooper, J. A. (1997). Mouse disabled (*mDab1*): a Src binding protein implicated in neuronal development. *Embo J* 16, 121-32.
- Kaletta, T., Schnabel, H., and Schnabel, R. (1997). Binary specification of the embryonic lineage in *Caenorhabditis elegans*. *Nature* 390, 294-8.
- Kimura, K. D., Tissenbaum, H. A., Liu, Y., and Ruvkun, G. (1997). *daf-2*, an insulin receptor-like gene that regulates longevity and diapause in *Caenorhabditis elegans*. *Science* 277, 942-6.
- Kmieciak, T. E., and Shalloway, D. (1987). Activation and suppression of pp60^{c-src} transforming ability by mutation of its primary sites of tyrosine phosphorylation. *Cell* 49, 65-73.
- Kokel, M., Borland, C. Z., DeLong, L., Horvitz, H. R., and Stern, M. J. (1998). *clr-1* encodes a receptor tyrosine phosphatase that negatively regulates an FGF receptor signaling pathway in *Caenorhabditis elegans*. *Genes Dev* 12, 1425-37.
- Kypta, R. M., Goldberg, Y., Ulug, E. T., and Courtneidge, S. A. (1990). Association between the PDGF receptor and members of the *src* family of tyrosine kinases. *Cell* 62, 481-92.
- Laemmli, U. K. (1970). Cleavage of structural proteins during assembly of the head Bacteriophage T4. *Nature* 227, 680-685.
- Laudano, A., and Buchanan, J. M. (1986). Phosphorylation of tyrosine with the carboxyl-terminal tryptic peptide of pp60^{c-src}. *Proc. Natl. Acad. Sci. USA*. 83, 892-896.
- L'Hernault, S. W., Shakes, D. C., and Ward, S. (1988). Developmental genetics of chromosome I spermatogenesis-defective mutants in the nematode *Caenorhabditis elegans*. *Genetics* 120, 435-52.
- Lin, R., Thompson, S., and Priess, J. R. (1995). *pop-1* encodes an HMG box protein

- required for the specification of a mesoderm precursor in early *C. elegans* embryos. *Cell* 83, 599-609.
- Lin, R., Hill, R. J., and Priess, J. R. (1998). POP-1 and anterior-posterior fate decisions in *C. elegans* embryos. *Cell* 92, 229-39.
- Lowell, C. A., and Soriano, P. (1996). Knockouts of Src-family kinases: stiff bones, wimpy T cells, and bad memories. *Genes Dev* 10, 1845-57.
- Matsuyoshi, N., Hamaguchi, M., Taniguchi, S., Nagafuchi, A., Tsukita, S., and Takeichi, M. (1992). Cadherin-mediated cell-cell adhesion is perturbed by v-src tyrosine phosphorylation in metastatic fibroblasts. *J Cell Biol* 118, 703-14.
- McKim, K. S., Howell, A. M., and Rose, A. M. (1988). The effects of translocations on recombination frequency in *Caenorhabditis elegans*. *Genetics* 120, 987-1001.
- Mello, C. C., Schubert, C., Draper, B., Zhang, W., Lobel, R., and Priess, J. R. (1996). The PIE-1 protein and germline specification in *C. elegans* embryos [letter]. *Nature* 382, 710-2.
- Morris, J. Z., Tissenbaum, H. A., and Ruvkun, G. (1996). A phosphatidylinositol-3-OH kinase family member regulating longevity and diapause in *Caenorhabditis elegans*. *Nature* 382, 536-9.
- Mulcahy, L. S., Smith, M. R., and Stacey, D. W. (1985). Requirement for ras proto-oncogene function during serum-stimulated growth of NIH 3T3 cells. *Nature* 313, 241-43.
- O'Farrel, P. H. (1975). High resolution two-dimensional electrophoresis of proteins. *J. Biol. Chem.* 250, 4007-4021.
- Papkoff, J., Rubinfeld, B., Schryver, B., and Polakis, P. (1996). Wnt-1 regulates free pools of catenins and stabilizes APC-catenin complexes. *Mol Cell Biol* 16, 2128-34.
- Papkoff, J. (1997). Regulation of complexed and free catenin pools by distinct mechanisms. *JBC* 272, 4536-4543.
- Piwnica-Worms, H., Saunders, K. B., Roberts, T. M., Smith, A. E., and Cheng, S. H. (1987). Tyrosine phosphorylation regulates the biochemical and biological properties of pp60c-src. *Cell* 49, 75-82.
- Powell-Coffman, J. A., Knight, J., and Wood, W. B. (1996). Onset of *C. elegans* gastrulation is blocked by inhibition of embryonic transcription with an RNA polymerase antisense RNA. *Dev Biol* 178, 472-83.
- Priess, J. R., and Hirsh, D. I. (1986). *Caenorhabditis elegans* morphogenesis: the role of the cytoskeleton in elongation of the embryo. *Dev Biol* 117, 156-73.
- Rocheleau, C. E., Downs, W. D., Lin, R., Wittmann, C., Bei, Y., Cha, Y. H., Ali, M., Priess, J. R., and Mello, C. C. (1997). Wnt signaling and an APC-related gene specify endoderm in early *C. elegans* embryos. *Cell* 90, 707-16.

- Rose, A. M., Baillie, D. L., and Curran, J. (1984). Meiotic pairing behavior of two free duplications of linkage group I in *Caenorhabditis elegans*. *Mol Gen Genet* 195, 52-6.
- Rose, L. S., and Kemphues, K. J. (1998). Early patterning of the *C. elegans* embryo. *Annu Rev Genet* 32, 521-45.
- Rubinfeld, B., Albert, I., Porfiri, E., Fiol, C., Munemitsu, S., and Polakis, P. (1996). Binding of GSK3 β to the APC-beta-catenin complex and regulation of complex assembly. *Science* 272, 1023-6.
- Rushforth, A. M., Saari, B., and Anderson, P. (1993). Site-selected insertion of the transposon Tc1 into a *Caenorhabditis elegans* myosin light chain gene. *Mol Cell Biol* 13, 902-10.
- Schaller, M. D., Hildebrand, J. D., Shannon, J. D., Fox, J. W., Vines, R. R., and Parsons, J. T. (1994). Autophosphorylation of the focal adhesion kinase, pp125FAK, directs SH2-dependent binding of pp60src. *Mol Cell Biol* 14, 1680-8.
- Sicheri, F., Moarefi, I., and Kuriyan, J. (1997). Crystal structure of the Src family tyrosine kinase Hck. *Nature* 385, 602-9.
- Simon, M. A., Drees, B., Kornberg, T., and Bishop, J. M. (1985). The nucleotide sequence and the tissue-specific expression of *Drosophila* c-src. *Cell* 42, 831-40.
- Smith, M. R., Degndicibus, S. J., and Stacey, D. W. (1986). Requirement for c-ras proteins during viral oncogene transformation. *Nature* 320, 540-43.
- Soriano, P., Montgomery, C., Geske, R., and Bradley, A. (1991). Targeted disruption of the c-src proto-oncogene leads to osteopetrosis in mice. *Cell* 64, 693-702.
- Stein, P. L., Lee, H. M., Rich, S., and Soriano, P. (1992). pp59fyn mutant mice display differential signaling in thymocytes and peripheral T cells. *Cell* 70, 741-50.
- Stein, P. L., Vogel, H., and Soriano, P. (1994). Combined deficiencies of Src, Fyn, and Yes tyrosine kinases in mutant mice. *Genes & Dev.* 8, 1999-2007.
- Steinbrich, R. (1993). FMOC peptide-resin cleavage, one simple approach to successful cleavage. Applied Biosystems/Perkin Elmer Publication.
- Sulston, J. E., Schierenberg, E., White, J. G., and Thomson, J. N. (1983). The embryonic cell lineage of the nematode *Caenorhabditis elegans*. *Dev Biol* 100, 64-119.
- Sundaram, M., and Han, M. (1996). Control and integration of cell signaling pathways during *C. elegans* vulval development. *Bioessays* 18, 473-80.
- Sundaram, M., Yochem, J., and Han, M. (1996). A Ras-mediated signal transduction pathway is involved in the control of sex myoblast migration in *Caenorhabditis elegans*. *Development* 122, 2823-33.
- Superti-Furga, G., and Courtneidge, S. A. (1995). Structure-function relationships in Src

family and related protein tyrosine kinases. *Bioessays* 17, 321-30.

Superti-Furga, G., and Gonfloni, S. (1997). A crystal milestone: the structure of regulated Src. *Bioessays* 19, 447-50.

Takahashi, F., Endo, S., Kojima, T., and Saigo, K. (1996). Regulation of cell-cell contacts in developing *Drosophila* eyes by Dsrc41, a new, close relative of vertebrate c-src. *Genes Dev* 10, 1645-56.

Takeya, T., and Hanafusa, H. (1983). Structure and sequence of the cellular gene homologous to the RSV src gene and the mechanism for generating the transforming virus. *Cell* 32, 881-90.

Talamonti, M. S., Roh, M. S., Curley, S. A., and Gallick, G. E. (1993). Increase in activity and level of pp60c-src in progressive stages of human colorectal cancer. *J Clin Invest* 91, 53-60.

Taylor, S. J., and Shalloway, D. (1994). An RNA-binding protein associated with Src through its SH2 and SH3 domains in mitosis. *Nature* 368, 867-71.

Thomas, J. H., and Inoue, T. (1998). Methuselah meets diabetes. *BioEssays* 20, 113-115.

Thorpe, C. J., Schlesinger, A., Carter, J. C., and Bowerman, B. (1997). Wnt signaling polarizes an early *C. elegans* blastomere to distinguish endoderm from mesoderm. *Cell* 90, 695-705.

Tsukita, S., Oishi, K., Akiyama, T., Yamanashi, Y., and Yamamoto, T. (1991). Specific proto-oncogenic tyrosine kinases of src family are enriched in cell-to-cell adherens junctions where the level of tyrosine phosphorylation is elevated. *J Cell Biol* 113, 867-79.

Verbeek, B. S., Vroom, T. M., Adriaansen-Slot, S. S., Ottenhoff-Kalff, A. E., Geertzema, J. G., Hennipman, A., and Rijksen, G. (1996). c-Src protein expression is increased in human breast cancer. An immunohistochemical and biochemical analysis. *J Pathol* 180, 383-8.

Weng, Z., Taylor, J. A., Turner, C. E., Brugge, J. S., and Seidel-Dugan, C. (1993). Detection of Src homology 3-binding proteins, including paxillin, in normal and v-Src-transformed Balb/c 3T3 cells. *J Biol Chem* 268, 14956-63.

Williams-Masson, E. M., Malik, A. N., and Hardin, J. (1997). An actin-mediated two-step mechanism is required for ventral enclosure of the *C. elegans* hypodermis. *Development* 124, 2889-901.

Wood, W. B. (1998). Handed asymmetry in nematodes. *Semin Cell Dev Biol* 9, 53-60.

Wu, H., Reynolds, A. B., Kanner, S. B., Vines, R. R., and Parsons, J. T. (1991). Identification and characterization of a novel cytoskeleton-associated pp60src substrate. *Mol Cell Biol* 11, 5113-24.

Yamaguchi, H., and Hendrickson, W. A. (1996). Structural basis for activation of human lymphocyte kinase Lck upon tyrosine phosphorylation. *Nature* 384, 484-9.

Zhang, X. (1996). . In Department of Biochemistry and Molecular Biology (Durham: University of New Hampshire).

Zwaal, R. R., Broeks, A., van Meurs, J., Groenen, J. T., and Plasterk, R. H. (1993). Target-selected gene inactivation in *Caenorhabditis elegans* by using a frozen transposon insertion mutant bank. *Proc Natl Acad Sci U S A* 90, 7431-5.

APPENDIX

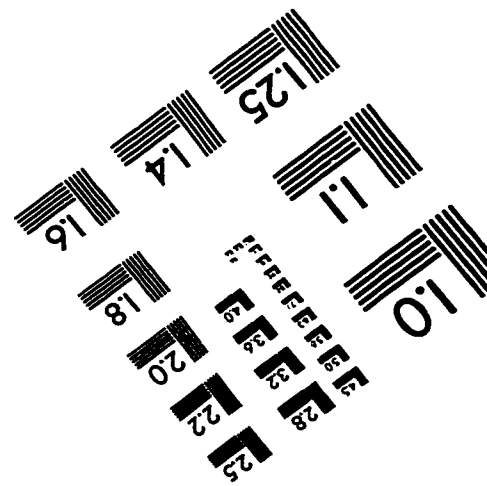
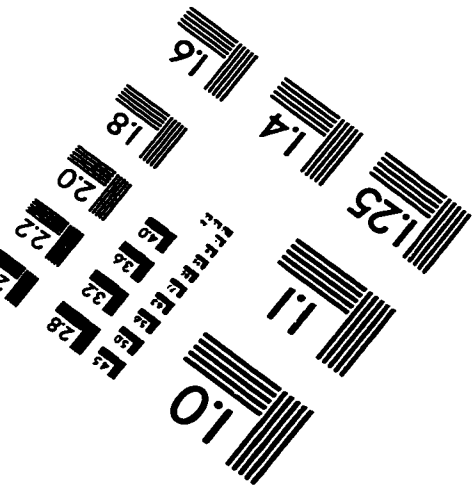
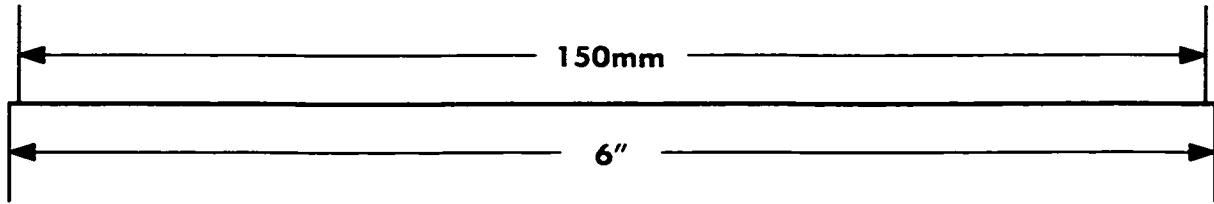
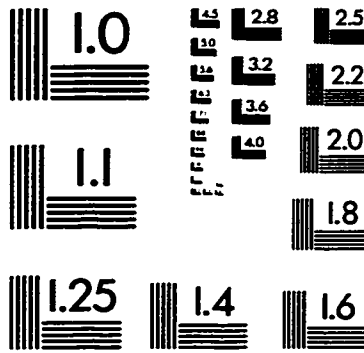
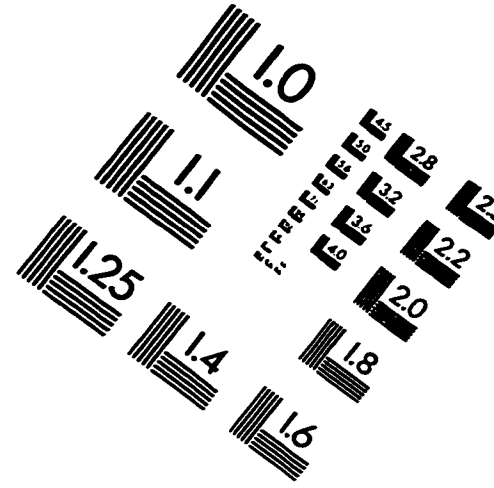
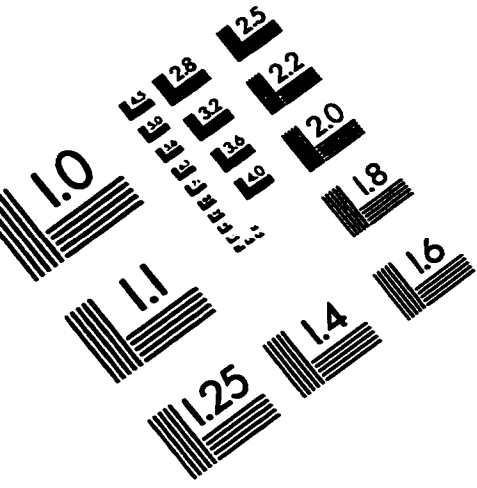
Abbreviations

AMP - ampicillin
3-AT - 3-amino-1, 2, 4-triazole
BSA - bovine serum albumin
DNA - deoxyribonucleic acid
DTT - dithiothreitol
EDC - 1-ethyl-3-(3-dimethyl-1-aminopropyl)-carbodiimide
EDT - 1,2-ethanedithiol
EDTA - ethylenediaminetetraacetic acid
EGF - epidermal growth factor
EGTA - ethylenebis(oxyethylenitrilo)tetraacetic acid
ELISA - enzyme linked immunosorbent assay
ENU - N-ethyl-N-nitrosourea
HRP - horseradish peroxidase
LB - luria broth
LiAc - lithium acetate
MtBE - methyl t-butyl ether
NGM - nutrient growth media
NHS - N-hydroxysulfosuccinimide
NP40 - nonidet P-40
PBS - phosphate buffered saline
PBST - phosphate buffered saline, Tween-20
PCR - polymerase chain reaction
PDGF - platelet-derived growth factor
PEG - polyethylene glycol 1500
PMSF - phenylmethylsufonyl fluoride
RNA - ribonucleic acid
RT-PCR - reverse transcription polymerase chain reaction
SC - synthetic complete
SDS - sodium dodecyl sulfate
TFA - trifluoroacetic acid
WLB - worm lysis buffer
YAC - yeast artificial chromosome

C. elegans Gene Names

abl = related to oncogene abl
age = ageing alteration
ama = amanitin resistant
apr = APC-related
bli = blistered cuticle
clr = clear
daf = abnormal dauer formation
dpy = dumpy
egl = egg-laying defective
hmp = humpback
hmr = hammer head
let = lethal
lin = abnormal cell lineage
lit = loss of intestine
lon = long
mom = more mesoderm
mut = mutator
ncl = abnormal nucleoli
par = partitioning-defective
pop = posterior pharynx defect
sem = sex muscle abnormal
sgk = shaggy/GSK3-related
sqt = squat
src = src oncogene related
unc = uncoordinated
wrm = worm arm motif

IMAGE EVALUATION TEST TARGET (QA-3)



APPLIED IMAGE, Inc
1653 East Main Street
Rochester, NY 14609 USA
Phone: 716/482-0300
Fax: 716/288-5989

© 1993, Applied Image, Inc., All Rights Reserved